MICROWAVE POWER TRANSMISSION FROM SPACE AND RELATED NONLINEAR PLASMA EFFECTS

HIROSHI MATSUMOTO

Abstract

We first present a brief historical review of the development of technology and scientific research related to the transmission of electrical energy via radio waves. The idea of radio power transmission was first conceived by Tesla about a century ago. However, the first practical use of radio waves was for transmitting intelligence and information, and not for transmitting electrical power per se. At the close of World War II, engineers and scientists re-examined the original Tesla idea of transmitting electric power to a distant place via radio, as high-power microwave technology became available. These efforts in 1960's resulted in the idea of the Solar Power Satellite (SPS) which was proposed by P. Glaser in 1968. The NASA/DOE concept of the SPS was extensively developed in the late 1970's. After reviewing the history of microwave power transmission and related theoretical/experimental studies from the beginning of this century up to 1980, we will discuss recent research on microwave power transmission after 1980. Our focus will be on related experiments conducted in the 1980's and 1990's, including those on ground-to-ground microwave energy transmission, ground-to-aircraft power transmission, and rocket-to-rocket power transmission. The rocket experiment we discuss was conducted to examine a possible nonlinear resonant interaction of intense microwaves with the ionospheric plasma. The result of the rocket experiment is further studied in detail by particle model computer simulations, and the results are explained in terms of nonlinear plasma effects. Such problems of interaction between the microwave power beam and the ionosphere must be resolved before space-to-ground and space-to-space power transmission can be realistically developed.

1. Introduction

On the occasion of the 75th Anniversary of URSI, it is appropriate to re-examine the historical traces of radio utilization for transmitting electric power without wires to a distant destination. Today, radio waves are mainly used for transmitting intelligence and information. However, the threat of the lack of energy resources, especially for electrical energy, is increasing as a result of

Prof. Hiroshi Matsumoto is with the
Radio Atmospheric Science Center
Kyoto University, Uji,
Kyoto 611, Japan
Tel: + 81 (774) 33 2532　　*Fax: + 81 (774) 31 8463*

the population explosion and rapid industrialization over the globe. Therefore, considering that the energy problem on our mother planet Earth, and the crisis of the Earth's environment have become urgent issues for mankind, we need to re-examine the use of radio waves for transmission of clean electrical energy from one place to another, especially from space to the ground, without wires.

There exists a good review paper by W. C. Brown [1] on the history up to 1980 of power transmission by radio waves. We briefly describe, in Section 2, the historical footprints of radio power transmission from a century ago to 1980. In the late 1970's, the NASA/DOE sponsored extensive studies on the Solar Power Satellite (SPS). The NASA/DOE SPS studies program contained an evaluation of the impact of a microwave power beam on the plasma environment of the ionosphere. Section 3 reviews the theoretical studies on Ohmic heating of the ionosphere, the thermal self focusing instabilities caused by the SPS microwave power beam and the related ionospheric heating experiments by ground-based heating facilities. Following these studies, the present author conducted a further study of microwave action on the ionospheric plasma, focusing on the nonlinear resonant scattering of the microwave power beam by magnetized ionospheric plasma. Section 4 presents a theoretical study of the nonlinear resonant interaction of a high-power microwave beam with ionospheric plasma, and a rocket experiment called MINIX (Microwave-Ionosphere Nonlinear Interaction eXperiment) which was conducted to test the theoretical estimate of nonlinear resonant interactions. Extensive computer simulations of nonlinear resonant interactions were carried out by the present author and his colleagues to interpret the MINIX result in terms of nonlinear wave-wave-particle interactions. Section 5 describes the computer simulation and its theoretical interpretation.

In Section 6 we outline two recent microwave-driven airplane experiments: SHARP in Canada and MILAX in Japan. The recent experiment on microwave power beam steering using an active phased array system developed in Japan is described as well. In Section 7 a brief account of a recent rocket experiment and recent ground-to-ground power transmission is given. In Section 8 we conclude with a summary and discussion for future plans of research and development on microwave power transmission (MPT).

2. History of microwave power transmission before 1980

In, 1864, James Clerk Maxwell [2] predicted the existence of radio waves by means of mathematical model. Twenty four years later, in 1888, bolstered by Maxwell's theory, Heinrich Hertz [3] first succeeded in showing experimental evidence of radio waves by his spark-gap radio transmitter. This experiment stimulated Marchese Guglielmo Marconi [4], who first achieved signal transmission by means of radio waves over 10 m in 1895, and over the Atlantic Ocean in 1901. It was Reginald Fessenden [5] who first succeeded in transmitting continuous wave (CW) for voice telecommunications [6]. Thus, the road to modern radio telecommunication was opened up around the turn of the century. Modern radio utilization has been directed into the area of radio telecommunications for transmission of "intelligence and information" over rather weak radio waves. This is one main stream of radio utilization stemming from the Maxwell-Hertz-Marconi-Fessenden work. However, another stream of work was directed toward a different radio wave application. The second stream of radio utilization was an effort to transmit electrical energy by radio to a distant place. These two streams are illustrated in Figure 1.

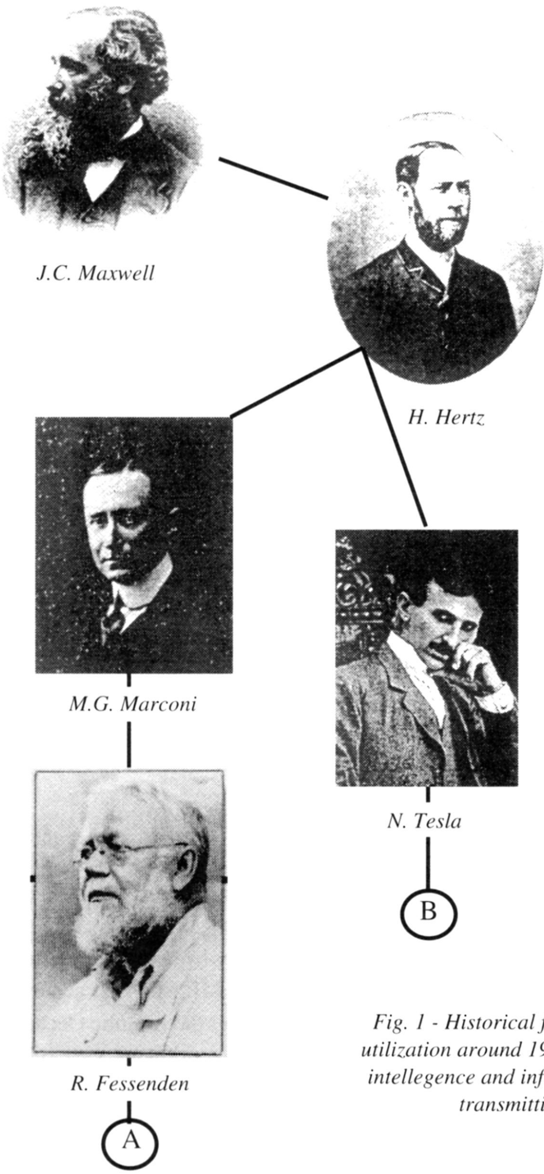

Fig. 1 - Historical figures along two stream lines of radio utilization around 1900. (A) is a line toward transmission of intellegence and information over radio, and (B) is toward transmitting electric power over radio

The idea of radio power transmission was first conceived and experimented on in 1899 by Nikola Tesla [7, 8]. He attempted to distribute ten thousand horse-power under a tension of one hundred million volts. He said "This energy will be collected all over the globe preferably in small amounts, ranging from a fraction of one to a few horse-power. One of its chief uses will be the illumination of isolated homes". He actually built a gigantic coil which was connected to a high mast of 200-ft with a 3 ft-diameter ball at its top (see Figure 2). He fed 300 kW power to the Tesla coil resonated at 150 kHz. The RF potential at the top sphere reached 100 MV.

From the turning point of the century on, however, radio has been used mainly for transmitting intelligence and information, and very few attempts have been made to transmit electrical energy over radio following Tesla's work.

The reason for a lack of interest in radio power transmission in the first half of this century is clear. People were waiting for the invention of a

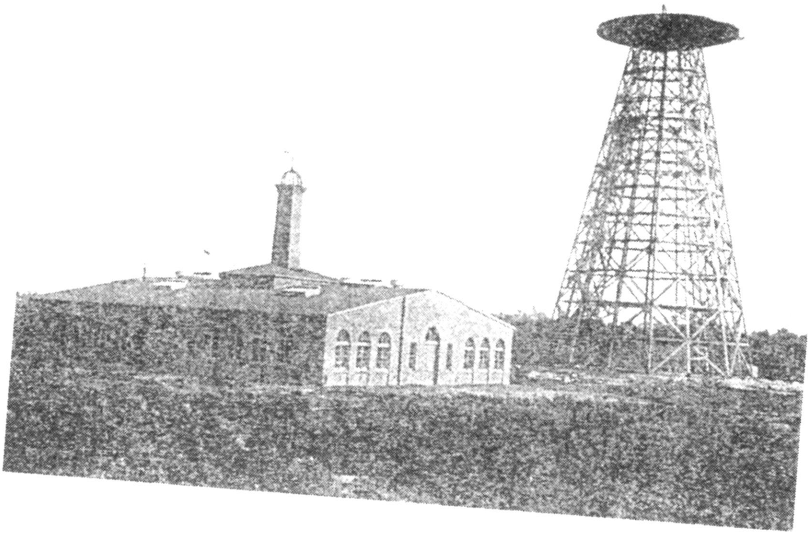

Fig. 2 - Tesla's experimental laboratory in Colorado Springs with power plant and transmitting tower [from N. Tesla, 1905]

high-power microwave device to generate electromagnetic energy of reasonably short wavelength, since efficient focusing toward the power receiving destination is strongly dependent on the use of technology of narrow-beam formation by small-size antennas and reflectors. In 1930's much progress in generating high-power microwaves was achieved by invention of the magnetron and the klystron. Though the magnetron was invented by A. W. Hull [9] in 1921, the practical and efficient magnetron tube gathered world interest only after Kinjiro Okabe [10] proposed the divided anode-type magnetron in 1928. It is interesting to note that H. Yagi and S. Uda[11], who are famous for their invention of Yagi-Uda Antenna, stressed a possibility of power transmission by radio waves in 1926, thereby displaying profound insight into the coming microwave tube era in Japan. Microwave generation by the klystron was achieved by the Varian brothers [12] in 1937 based on the first idea by the Heil brothers in Germany in 1935.

During World War II, development of radar technology accelerated the production of high-power microwave generators and antennas. A CW high power transmission over a microwave beam was investigated in secrecy in Japan. The project , the "Z-project" , was aimed at shooting down air-bombers by a high-power microwave beam from the ground, and involved two Nobel winners H. Yukawa and S. Tomonaga [13]. Figure 3 shows a 100 kW magnetron developed at that time, and an introduction of the Japanese Magnetron appeared in "Electronics" of USA immediately after World War II. However, the technology of the high-power microwave tube was still not developed sufficiently for the practical continuous transmission of electric power. Further, no power device was available to convert a microwave energy beam back to DC power until the 1960's.

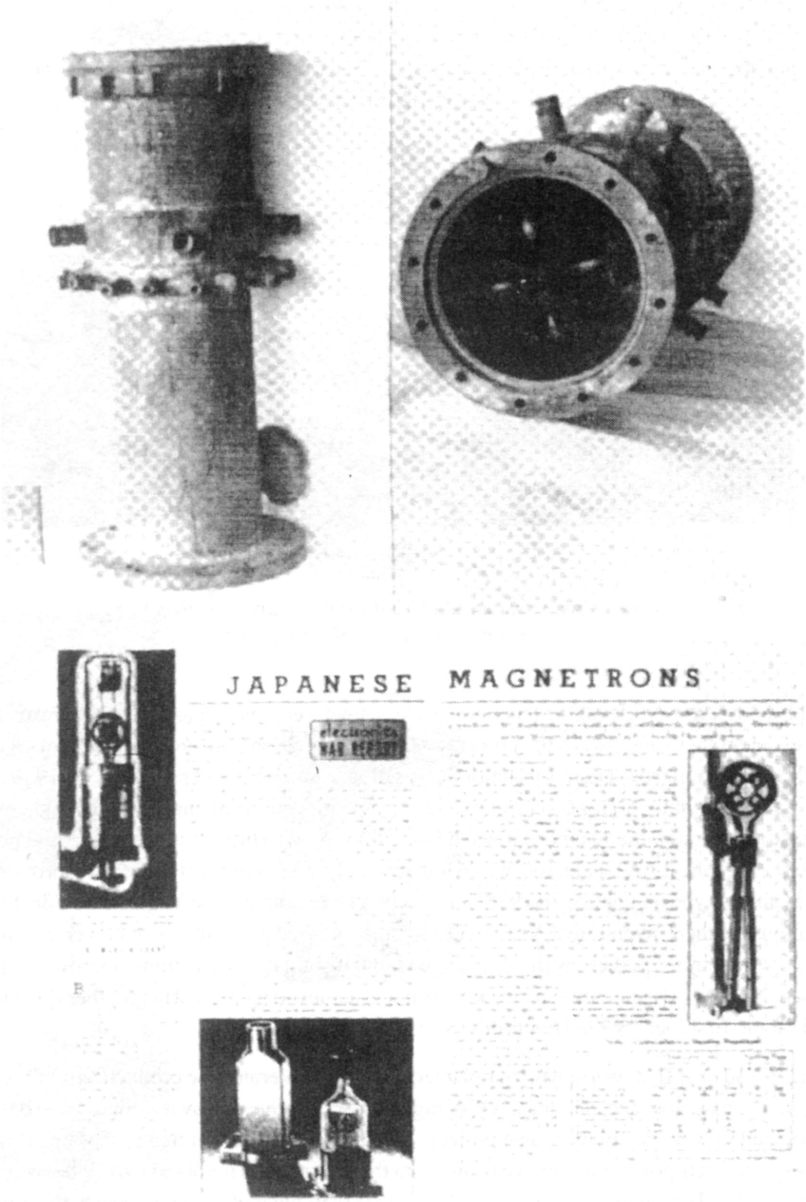

Fig. 3 - A 100 kW magnetron developed during World War II in Jaspan and a copy of an article appeared in US "Electronics" based on the onformation collected by US GHQ after the end of World War II

The post-war history of research on free-space power transmission is well documented by William C. Brown [1], who was a pioneer of practical microwave power transmission (see references in [1]). It was he [14] who first succeeded in demonstrating a microwave-powered helicopter in 1964, using 2.45 GHz in the frequency range of 2.4 - 2.5 GHz reserved for the ISM (Industrial, Scientific and Medical) applications of radio waves (see Figure 5 in [1]). A power conversion device from microwave to DC, called a rectenna, was invented [15, 16, 17] and used for the microwave-powered helicopter. The first rectenna (shown in Figure 3 in [1]) was composed of 28 half-wave dipoles terminated in a bridge rectifier using point-contact semiconductor diodes. Later, the point contact semiconductor diodes were replaced by silicon Schottky-barrier diodes which raised the microwave-to-DC conversion efficiency from 40 % to 84 %[1], the efficiency being defined as the ratio of DC output to microwave power absorbed by the rectenna. The highest record of 84% efficiency was attained in the demonstration of microwave power transmission in 1975 at the JPL Goldstone Facility [18]. Power was successfully transferred from the transmitting large parabolic antenna dish to the distant rectenna site over a distance of 1.6 km. The DC output was 30 kW [18] (see Figure 9 in [10]).

An important milestone in the history of microwave power transmission was the three-year study program called the DOE/NASA Satellite Power System Concept Development and Evaluation Program, started in 1977. This program was conducted for the study of the Solar Power Satellite (SPS), which is designed to beam down the electrical power of 5 to 10 GW from one SPS toward the rectenna site on the ground.

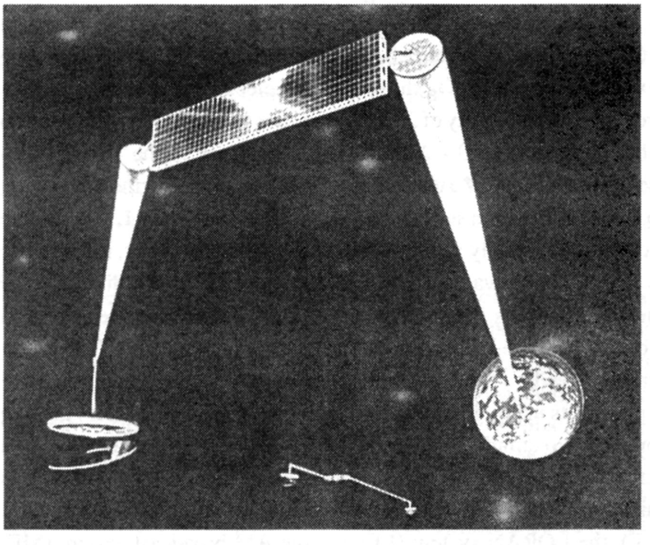

Fig. 4 - Artist concept of Solar Power Satellite. The power station will transmit electric power to the Earth and possibly to Space Factory, Space Farms and Space Cities in addition

The extensive study of the SPS ended in 1980, producing a 670 page summary document [19]. The concept of the SPS was first proposed by P. E. Glaser [20] in 1968 to meet both space-based and earth-based power needs. An artist's SPS concept is shown in Figure 4. The SPS will generate electric power of the order of several hundreds to thousands of megawatts using photo-voltaic cells of sizable area, and will transmit the generated power via a microwave beam to the receiving rectenna site. Among many technological key issues which must be overcome before the SPS realization, microwave power transmission (MPT) is one of the most important key research issues. The problem contains not only the technological development of microwave power transmission with high efficiency and high safety, but also scientific analysis of microwave impact onto the space plasma environment. We discuss this in the following three Sections.

3. Review of ohmic heating of the ionospere and thermal self-focusing instability by SPS and a related ionospere heating experiment

The SPS studies program, carried out in the latter half of 1970's under the sponsorship of the US NASA/DOE, contained research on the effects associated with the propagation of intense microwave beams through the ionosphere. Two main effects were pointed out.

The first is the resistive (Ohmic) heating effect due to collisional damping of microwaves. Though the fraction of wave energy absorbed by the ionospheric plasma is very small, the resultant Ohmic heating can significantly modify the local ionospheric thermal balance [21, 22]. The electron temperature is determined by a balance between heating and cooling processes. The heating by microwaves is proportional to square of the electric field of the microwave E^2, to square of the ratio of the local plasma frequency and the microwave frequency, $(f_p < f)^2$and to the collision frequencies ν_{ei} and ν_{en} where ν_{ei} and ν_{en} are the collision frequencies of electrons with ions and neutral particles, respectively. The collision frequency ν_{en} increases as the electron temperature increases. Thus Ohmic heating by intense microwaves can be self-amplifying, and thereby result in thermal runaway [22, 23]. Calculation of the balance between the enhanced heating and cooling losses through vibrational excitation of N_2 and O_2 shows that the electron temperature will be raised several-fold for a microwave power density of 23 mW/cm^2. It is also found that the electron density in the E-layer will be increased by 10 - 20 % due to a decrease in the temperature-dependent recombination rate of O_2^+ and NO_2^+, while in the D-layer increase in the attachment rate to O_2^+ will cause up to a 50 % reduction in the electron number density [21, 23]. As the ionospheric heating efficiency varies inversely as the square of the radio frequency, ionospheric heating equivalent to that by the SPS microwave beam can be achieved at lower radiated power by heating at a lower frequency. With this idea, experimental tests of the enhanced electron heating theory were carried out by the Rice University Group lead by W. E. Gordon [24], using the 430 MHz radar system at the Arecibo Observatory. A series of underdense $(f_{heater} < f_p)$ HF ionospheric modification experiments using the Platteville high power HF (5-10 MHz) heating facility at Colorado were conducted to simulate the effects of the SPS microwave beam, while monitoring potential impact upon telecommunication system performance [25, 26]. It was concluded that there is no significant difference between the telecommunication system performance of the OMEGA system (VLF), the LORAN system (LF) and the AM broadcast system (MF) between the times when the heating facility was operating and when it was not. Thus, the impact of the SPS intense microwave beam on the performance of VLF, LF and MF telecommunication systems would be minimal [25].

The second potential effect of the SPS microwave beam onto the ionosphere, studied extensively in the late 1970's, is the phenomenon of thermal self-focusing [27, 28, 29]. Thermal self-focusing takes place as a result of a positive feedback loop. Small natural density fluctuations in the ionosphere cause a spatial variation of the refractive index thereby giving rise to a slight focusing and defocusing of the microwave. This slight inhomogeneous (differential) heating of the ionospheric plasma results in a temperature gradient driving the plasma from the focused region and thereby amplifying the initial density fluctuations. The self-focusing instability will eventually reach a hydrodynamic equilibrium creating large-scale ionospheric irregularities. A self-focusing experiment was conducted at the Arecibo Observatory using intense HF electromagnetic wave under the overdense condition ($f_{heater} < f_p$) [30]. The experimental result showed clear self-focusing striations and large-scale structuring of the ionosphere. However, it is noted that these experiments were all conducted under the overdense condition and not the underdense condition.

The two main effects described above are caused basically by the non-resonant heating of the plasma by the intense electric field of the SPS microwave. Resonant interactions of the microwave beam with the ionospheric plasma are another interesting research area. Parametric excitation of ionospheric plasma waves was studied for multiple-frequency electromagnetic radiation. The interaction between two high frequency microwaves and a multiple of the ionospheric resonant frequency (such as the electron plasma frequency) was studied [31, 32] utilizing a model of an up-going pilot microwave signal operating at a frequency slightly separated from the downcoming power beam, and beat waves generated within the finite width of the main downcoming energy beam.

The US government suspended the NASA/DOE program study partly due to budget problems and partly because of the apparent recovery from the oil shock in the 1970's, although the NASA/DOE final report concluded that "no factors that would preclude the SPS research and development are found in the light of the highly potential future energy crisis".

4. Theory and rocket experiment (MINIX) on nonlinear plasma wave excitation by microwave power beam in the ionosphere

Most of the experiments conducted in the 1970's on the potential impact of the SPS microwave onto the ionosphere were conducted by the ground-based heating facility using much lower frequency than the SPS microwave frequency of 2.45 GHz. Therefore, the realistic resonant interaction of the SPS microwave with natural resonance frequency bands of the order of several MHz to several kHz may not have been adequately estimated. The resonant interaction naturally involves electrostatic waves which can be detected much more easily by in-situ measurement than by ground-based radar diagnostics. Based on such idea, an in-situ rocket experiment of radiating an intense 2.45 GHz microwave into the ionospheric plasma was proposed by the present author in the early 1980's in Japan. The project was named MINIX which stands for Microwave Ionosphere Nonlinear Interaction eXperiment.

The plasma response to the injected microwave power beam was monitored by diagnostic sensors and receivers onboard the rocket. Preceding the MINIX experiment, Matsumoto [33, 34] numerically evaluated the growth rate of the resonant instabilities of electron plasma waves and ion acoustic waves as a result of Raman and Brillouin scattering of the SPS intense microwave under model ionospheric plasma parameters. The growth rate of Langmuir waves as a result of the Raman scattering of the microwave is given [34] by

$$\gamma_e = -\frac{1}{2}\left[\Gamma_e + \Gamma_2 - \sqrt{(\Gamma_e + \Gamma_2)^2 + \frac{\Pi_e^2}{\omega^2} k^2 v_0 \sin^2 \varphi}\right] \tag{1}$$

where Π_e is the electron plasma frequency and Γ_e is the damping rate of Langmuir waves; the latter includes two terms resulting from the Landau damping and collisional damping. The quantity Γ_2 represents a collisional damping of the back-scattered microwave with a frequency of

$$\omega_2 = \sqrt{\Pi_e^2 + c^2 (k - k_0)^2}$$

$v_0 = eE_0 / (m_e \omega_0)$ is the sloshing velocity of electrons by the SPS microwave, and φ is an angle between k and E_0. The suffix o denotes the quantity associated with the SPS microwave. A similar expression for the growth rate Γ_i for ion acoustic waves was also obtained [34] (not shown). Numerical calculation of Γ_e and Γ_i versus the ionospheric altitude (see Figure 5) showed that Langmuir waves are easily excited by the SPS microwave, while the growing time of ion acoustic

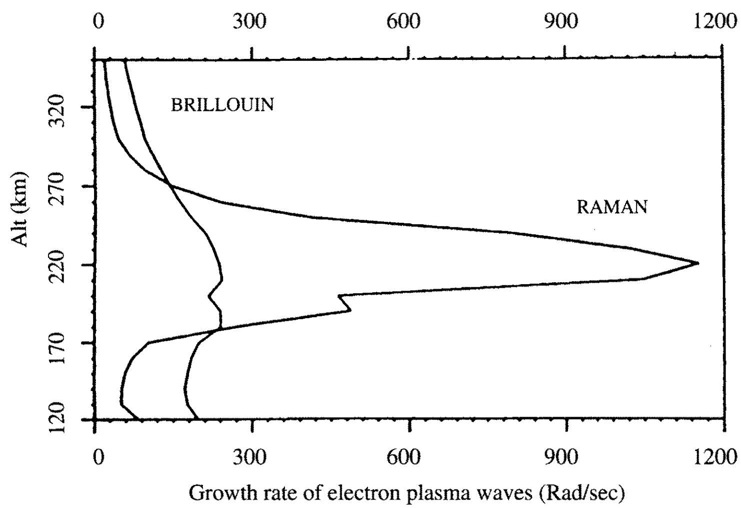

F ig. 5 - Growth rates of Langmuir waves excited by the Roman scattering of the SPS microwave, and fo ion acoustic waves excited by the Brillouin scattering of the SPS microwave. The microwave field E_0 is assumed to be 220 V/m (from [33]).

waves is much slower. It is noted that the growth rate expression (1) gives only the initial growth rates as a result of nonlinear interaction between the three waves: the incident intense microwave, the back-scattered microwave and the excited Langmuir wave. The nonlinear coupling of the three waves should satisfy both energy and momentum conservation in the form of

$$\omega_0 = \omega_1 + \omega_2 \cdot \boldsymbol{k}_0 = \boldsymbol{k}_1 + \boldsymbol{k}_2 \tag{2}$$

where ω_j and k_j (j=0, 1, 2) are angular frequency and wave number respectively, and the subscripts 0, 1 and 2 represent the incident microwave, the back-scattered microwave, and the excited Langmuir wave, respectively.

The MINIX rocket experiment was carried out by a Japanese sounding rocket S-520-6 of ISAS (Institute of Space and Astronomical Sciences) on August 29 in 1983 [35, 36, 37, 38]. The experiment was conducted with a mother-and-daughter rocket system. Figure 6 shows an artist's concept of the experiment, while Figure 7 represents the ground testing of the mother-daughter system with the real flight model payloads. Two sets of high power (~ 830 watts) magnetrons (reinforced versions of Toshiba Magnetron 2M172 for home use oven) were installed on the mother section of the rocket payload and were connected to the truncated waveguide antenna (see

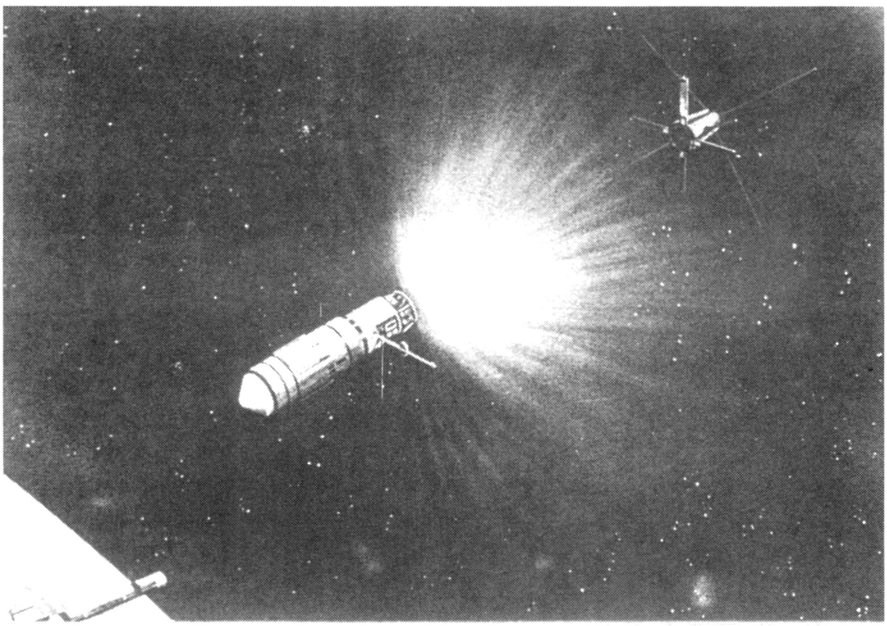

Fig. 6 - An artist concept of the MINIX rocket experiment. A high power microwave (~ 830 watts) was radtiated from the truncated wave guide antenna toward the daughter rocket section by which the nonlinear responses of the ionospheric plasma were measured.

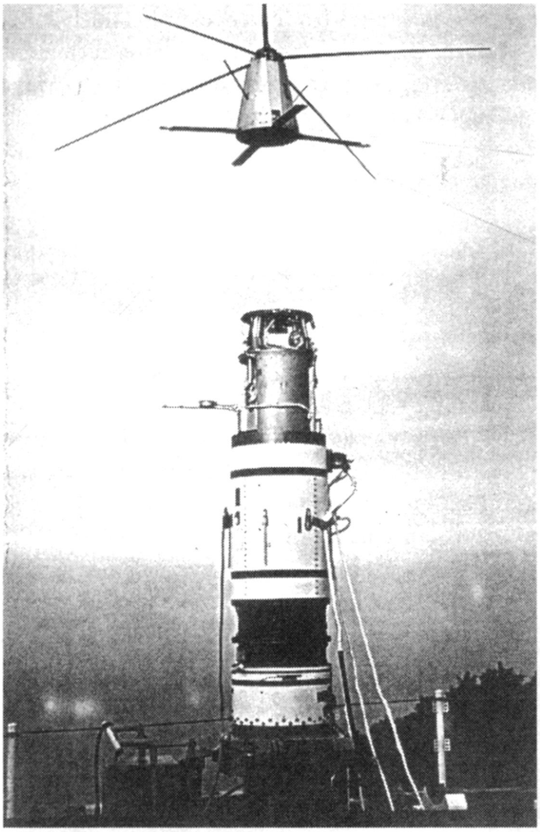

Fig. 7 - A photograph of pre-flight test scene of the MINIX payload at launching site KSC in Japan. The daughter unit with various sensors and diagnostic packages was separated by a crane from the mother section. A truncated wave guide antenna used for the side ward transmission is seen in the mother section

Figure 8) to radiate intense microwave with a frequency of 2.45 GHz. The DC power supply to the magnetrons was given by onboard batteries. A plasma diagnostic package was installed on the daughter unit of the rocket. It was composed of a VLF wide band receiver, an HF sweep frequency receiver, a geomagnetic aspect sensor, electron density and temperature meter, and a microwave receiver. Four rod antennas with a length of 2 m were extended out from the daughter rocket in the top plane of the daughter unit to detect plasma waves which are expected to be nonlinearly excited by the injected intense microwave. The HF sweep frequency receiver covered a frequency range from 100 kHz up to 18 MHz with a sweeping time of 250 msec. The VLF receiver covered a frequency range from 60 Hz up to 25 kHz. Four paddles were extended out at the bottom level of the daughter unit and were used for rectennas. The

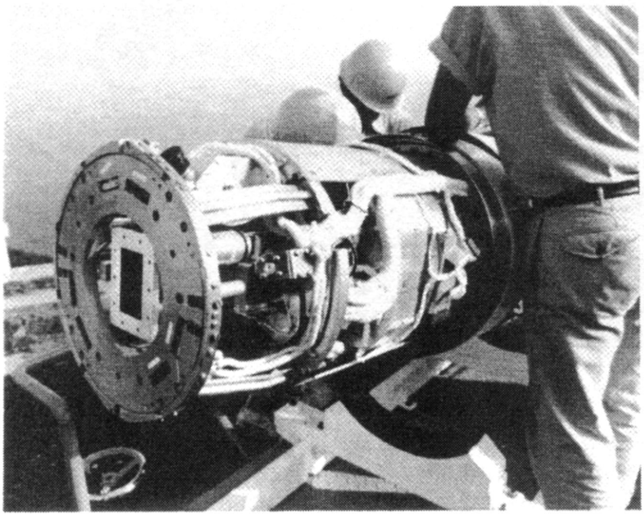

Fig. 8 - The truncated wave guide antenna aperture used for the forward transmission of 2.45 GHz microwave onboard the MINIX payload.

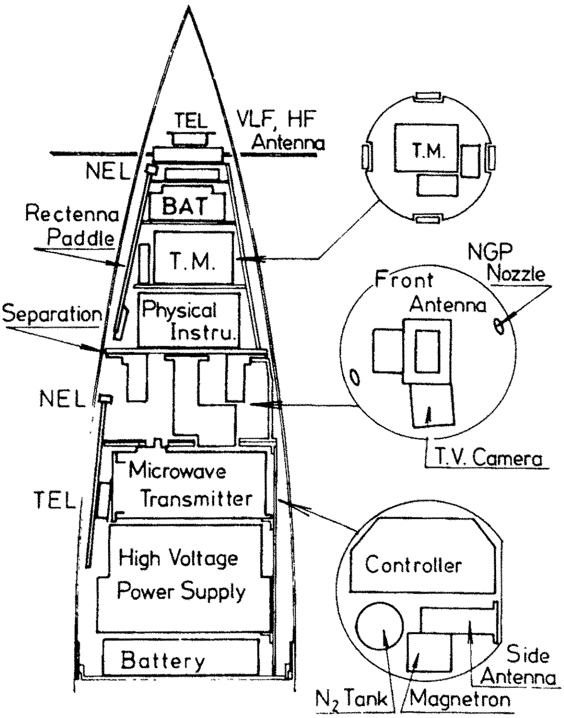

Fig. 8 - Payload configuration of MINIX rocket experiment. Mother and daughter sections are separated by spring coil during the flight in the ionosphere

arrangement of these antennas and paddles is shown in Figure 7. Figure 9 shows the configuration of the payload instrumentation on board S-520-6 rocket. The mother unit, which is the section below the level of separation plane in Figure 9, carried the power supply composed of the DC-battery and DC-DC converter, the microwave transmitter with a time sequencer, two sets of truncated wave guide antennas, a Langmuir probe, a wide-band telemetry set, a neutral gas plume of N_2 gas, and a TV monitor camera for monitoring the in-flight separation of the daughter unit. The neutral gas plume was prepared to create an artificially simulated D-layer with high collision frequency at the height of the lower F layer near the apex of the rocket orbit.

Figure 10 shows the trajectory of the S-520-6 rocket. The MINIX experimental time sequence along the orbit is also shown in the figure. The thick line parts along the orbit indicate the time interval of microwave transmission. The experiment was conducted under three different modes: The first mode (I) was devoted to the study of Ohmic heating in the ionospheric D-layer and lower E-layer. In this experimental mode, the microwave was transmitted continuously for a long duration of 10 seconds. Above the altitude of 100 km, the second mode (II) was in operation where the microwave was transmitted intermittently with a 5 sec transmission followed by a 5 sec pause-of-transmission period for the measurement of the plasma response. Under the mode (II), the microwave was radiated radially, i.e., in the direction perpendicular to the spin axis of the rocket. After the separation of the daughter unit near the apex of the orbit around 220 km altitude, the experimental mode was switched to the mode (III) where the

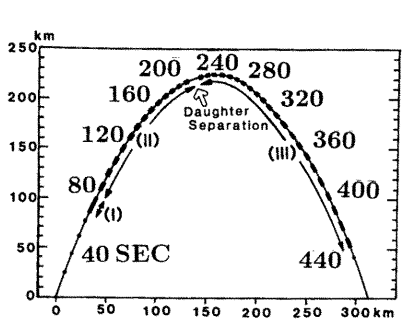

Fig. 10 - The trajectory of S-520-6 rocket and the time sequence of the MINIX along the orbit

microwave was transmitted forward in the axial direction from the truncated wave guide antenna facing the leaving daughter unit (see Figure 6), with the same ON-OFF time sequence as that in the mode II. The modes (II) and (III) were mainly prepared to detect the theoretically predicted excitation of plasma waves through nonlinear resonant interaction of the transmitted intense microwave.

All of the instrumentation on board the MINIX rocket worked perfectly and provided useful data. The measurement of the variation of electron temperature showed no temperature difference between ON and OFF periods of the microwave transmission during the mode (I). It turned out later with the use of pre-launch plasma chamber data on plasma heating by MINIX transmitter [39] that the estimated maximum temperature increase due to the Ohmic heating for the MINIX situation is below 100 K which is lower than the detectable limit by the Langmuir probe used in the MINIX. It is also noted that the effective time of microwave exposure to the ionospheric plasma particles was too short compared to the characteristic time for the Ohmic heating. The plasma volume illuminated by the intense microwave with a power density which is comparable to or higher than that of the SPS microwave is limited to within the distance of 2 m from the center of the truncated wave guide antenna. The power density and the electric field intensity of the microwave radiated by the magnetron plus wave guide antenna system are shown in Figure 11.

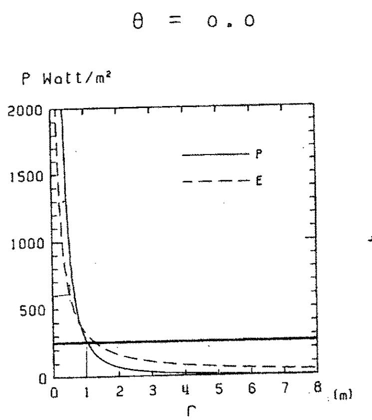

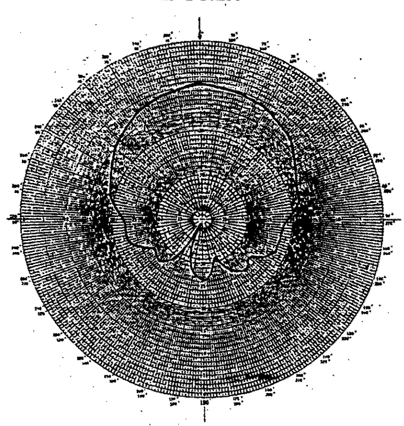

Fig. 11 - Power density and electric field intensity of the radiated microwave as a function of distance from the MINIX truncated wave guide antenna. The right panel shows the antenna pattern of the transmitting antenna.

The sweep frequency analyzer (SFA) in the HF range measured the spectrum of ionospheric plasma waves and broadcasting waves reaching the rocket altitude from the ground. The SFA detected strong plasma waves at certain frequency bands when and only when the microwave was transmitted. The plasma wave spectra from 100 kHz to 18 MHz are shown in Figure 12. The upper

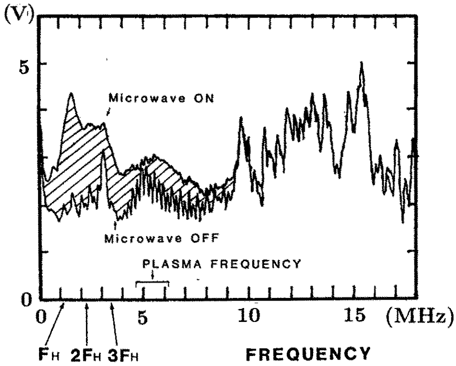

Fig. 12 - Plasma wave spectra observed by HF wave receiver onboard the daughter unit of the MINIX rocket experiment. The upper spectral line is for the time when the intense 2.45 GHz microwave is transmitted into the ionospheric plasma. The lower spectral line is for the time when the microwave is not transmitted. The spectral peaks above 10 MHz are due to the broadcasting waves reaching from the ground.

spectral curve is for the period of the microwave transmission, while the lower is for the no-transmission period. The spectra above 10 MHz are not different from each other, but those below 10 MHz show a clear difference. The shaded part shows the enhancement of the spectral components due to additional excitation of the plasma waves by the intense microwave. In Figure 12, the local electron cyclotron frequency F_H and its harmonics and the local electron plasma frequency are indicated on the horizontal frequency axis. The error bar in the electron plasma frequency was due to the ambiguity in determining the number density and temperature from the Langmuir probe. The enhancement in the spectral intensity is seen in two different characteristic frequency ranges. One is seen at odd half harmonics of the local electron cyclotron frequency in the range from 1.5 MHz to 3.5 MHz. The frequency range of these waves did not change with altitude as the local electron cyclotron frequency is almost constant in the orbit range of the rocket. Taking into account the observed frequency range and discrete peaks at odd half cyclotron frequencies, we explained these waves in terms of electron cyclotron harmonic (ECH) waves. The other enhancement is seen above the local electron plasma frequency ranging from 5 MHz to 8 MHz. The frequency range shifts upward with the altitude of the rocket, and accordingly with the increasing plasma density in the E- to F-layers of the ionosphere. We explained the enhancement of this frequency above the local electron plasma frequency in terms of Langmuir waves due to the excitation by the intense microwave through Raman scattering.

The VLF wide band receiver could not pick up the expected ion acoustic wave through Brillouin scattering. This was not surprising because the theoretically calculated [34] growth rate of the ion acoustic waves is not large enough to make these waves grow to the observable amplitude within a short time illuminated by the microwave at a fixed point of the ionosphere. The illuminated time was about 1 msec, which is calculated by the size of the plasma volume illuminated by the intense ($E > 200$ V/m) microwave, while the theoretically calculated growing time is longer than 10 msec.

The result of the MINIX on nonlinear plasma wave excitation due to intense 2.45 GHz microwaves was not much different from what had been predicted by the theoretical calculation. A similar but more complicated expression of the growth rate of the electron cyclotron waves including upper hybrid waves was obtained based on the nonlinear kinetic theory of resonant three-wave coupling[40, 41]. It is expressed as

$$\gamma_{ECH} = \sqrt{|\beta_1 \beta_2|} E_0 \tag{3}$$

where E_0 is the intensity of the incident intense microwave, and β_1 and β_2 are the coupling coefficients defined by

$$\frac{dE_1}{dt} = i\beta_1 E_2^* E_0 \tag{4}$$

$$\frac{dE_2}{dt} = i\beta_2 E_0 E_1^* \tag{5}$$

where E_1 and E_2 are the electric field of the backscattered microwave and the excited electron cyclotron wave. With a lengthy calculation and by use of the resonant condition (2), we obtain the final complicated expression of β_1 and β_2 (eqs. (80) - (93) in [41]) which contains both tensor elements of the linear dispersion relation and the integral containing resonant terms at higher harmonics of electron cyclotron frequencies. Numerical calculation of the growth rate shows that the electron cyclotron harmonic waves are also excited by the intense microwave under ionospheric conditions.

Despite the qualitative agreement with these theoretical predictions, the MINIX result showed the following features which are not consistent with the above theory. The first point is that the observed spectrum of the excited Langmuir waves are not monochromatic, nor quasi-monochromatic, but of broad-band nature in contrast to the monochromaticity predicted by theory based on the resonance condition (2). The second point is that the intensity of the electron cyclotron waves is higher than the Langmuir wave intensity. The second point clearly contradicts the theoretical prediction. The saturation level of the nonlinearly excited plasma waves (both Langmuir and ECH waves) through the nonlinear resonant three wave-coupling is proportional to the growth rate divided by the product of the coupling coefficients $\beta_0 \beta_1$. The theory shows that the saturation level of the Langmuir waves should be larger than that of the ECH waves. However, the amplitude of the Langmuir waves excited by the microwave in the MINIX was smaller than that of the ECH. Thus, these two experimental features are not well explained by the conventional nonlinear resonant three-wave coupling theory. In the next section, we will describe our attempt to overcome this contradiction by the help of computer simulations.

5. Computer Simulation of Nonlinear Interaction of Microwave Power Beam with Space Plasma

Traditionally, methods of scientific research have involved a mutual interplay between experiment and theory. Experiment attempts to collect "factual" information through repeated or controlled measurements. Theory, on the other hand, tries to order accumulated factual knowledge and thereby propose a new paradigm of description of physical processes. New theoretical descriptions and new experiments challenge each other in turn. Such feedback between theory and experiment is generally on-going. However, as in the case of MINIX, theory and experiment sometimes show a gap which cannot be easily overcome because of difficulties of repeated experiments and/or a limit to the applicability of theory for highly nonlinear and complex processes. In order to fill such a gap, a third new approach become available with the advent of modern high speed computers. This third approach is called computer simulation or computer experiment. The basic idea of computer simulation is to simulate the physical behavior of complicated natural systems by solving an appropriate set of mathematical equations based on an accepted and fundamental physical mathematical model. As one can easily change the set of the mathematical equations as well as the boundary and initial conditions, the computer simulation can be a perfectly controlled experiment. The main advantage of computer simulations is that complicated physical systems including nonlinearity and/or strong inhomogeneity can be dealt with as easily as simpler, linear and homogeneous systems can be treated. The International Union of Radio Science (URSI) has played a significant role of accelerating the establishment of this third research tool in Radio Science, especially in the field space plasma wave studies through its activities in Commission H [43].

In order to understand the MINIX result and the nonlinear interaction of the intense microwave power beam with the ionospheric plasma (which contradicts the nonlinear resonant three wave coupling theory) we performed a series of computer simulations. The computer code used for this purpose is a particle-model simulation code called KEMPO [43]. KEMPO solves Maxwell's equations and simultaneous equations of motion of several tens of thousands to several millions of super-particles. The one-dimensional version of the KEMPO code is now available in the public domain [42]. As the MINIX result showed that there exist two different electrostatic (ES) plasma waves with two different propagation angles relative to the geomagnetic field, we have set up two different simulation models. One is the case where all of the incident intense microwave (or the "pump" electromagnetic (EM) wave in terms of nonlinear resonant three-wave coupling), the back-scattered microwave (or the back-scattered "idler" EM wave) and the excited ES plasma wave are assumed to propagate along the external magnetic field B_0. The other model assumes that they propagate in a perpendicular direction to B_0. The former and the latter cases are referred to as the "parallel case" and the "perpendicular case" hereafter. The energy and momentum conservation relation expressed by Eq.(2) can be graphically shown by a parallelogram in the ω-k diagram. Figure 13 is one example of the parallelogram in the perpendicular case. The common simulation parameters for both cases are listed in Table 1. Figure 14 shows an example of a temporal variation of the excited ES wave intensity, and that of the kinetic energy of electrons for both the parallel and perpendicular cases. The upper and lower panels correspond to the parallel and perpendicular cases, respectively. In the parallel case, an L-mode EM wave is adopted as the pump. The L-mode wave couples with a back-scattered L-mode EM wave and a Langmuir wave (LW). This coupling is referred to as L-L-LW coupling. A similar result is obtained (not shown) for R-R-LW wave coupling with the R-mode pump wave. In the perpendicular case, an X-mode EM wave is used as the pump. The X-mode pump wave is scattered producing a back-scattered X-mode EM and the ES ECH wave through the X-X-ECH coupling. A similar result is obtained for the O-O-ECH coupling (not shown). The ECH wave excited by the X-mode EM

Fig. 13 - A parallelogram in the ω-k diagram showing the resonant interaction between two electromagnetic waves (microwaves) and electron cyclotron harmonic (ECH) wave.

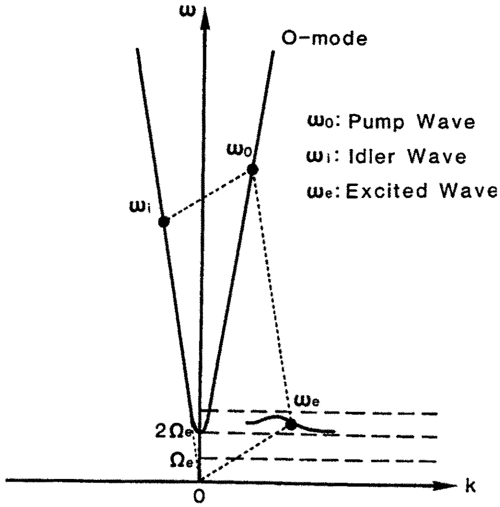

wave, shown in the lower panel, is one of the multiple harmonic modes of ECH waves. It is the upper hybrid mode that shrinks to the upper hybrid oscillation when its wave number tends to zero. As seen in Figure 14, both the LW and ECHW grow exponentially in the early phase. The numerically measured growth rates of the LW and ECHW are $\gamma_{LW} = 0.07$ and $\gamma_{LW} = 0.04$, respectively. These growth rates agree well with the theoretically predicted value of the growth rate based on the nonlinear resonant three-wave coupling theory.

In contrast to a good agreement of the growth rates of both LW and ECHW, the saturation levels of the LW and of the ECHW contradict the theoretical prediction as seen in Figure 14. The LW saturation level is almost half of that of the ECHW. The simulation result does not agree with theory, but agrees well with the result of the MINIX rocket experiment. Thus, the computer simulation could reproduce the inconsistency between the rocket experiment and theory. One of the merits of computer simulations is that one can make the diagnostics as detailed as one wishes from the information stored in memory. In particular, compared with rocket experiments, one can

<Plasma Parameters>

Speed of Light	c	50
Electron Plasma Angular Frequency	Π_e	2.0
Electron Cyclotron Angular Frequency	Ω_e	1.0
External Magnetic Field Strength	B_{ext}	1.0
Charge to Mass Ratio of Electrons	q_e/m_e	-1.0
Total Number of Electrons	N_p	32768
Parallel Thermal Speed of Electrons	$v_{th\parallel}$	1.0
Perpendicular Thermal Speed of Electrons	$v_{th\perp}$	1.0
Dielectric Constant	ε_0	1.0

<System Parameters>

Time Step	Δt	0.01
Grid Spacing	Δx	1.0
Number of Grids	N_x	2048

<Parameters of Injected EM Wave>

Angular Frequency	ω_0	18.5~23.4
Wave Number (Mode Number)	k_0	15~19
Wave Magnetic Field Strength	B_ω	0.5

Table 1 - Numerical parameters for simulations presented in Figure 14

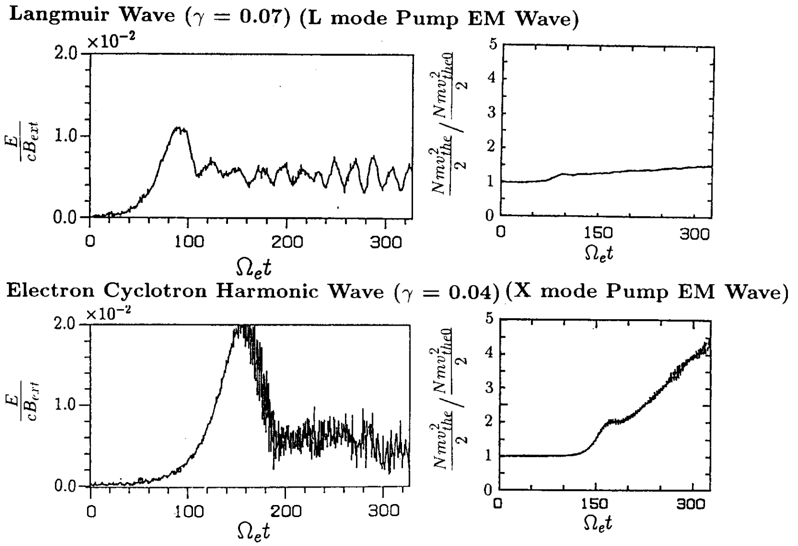

Fig. 14 - The left column shows time evolution of the electric field of electrostatic (ES) plasma waves excited nonlinearly by the pump electromagnetic (EM) waves. The right column shows the corresponding time history of particle thermal energy. The upper and lower panels are for the parallel and perpendicular cases, Langmuir Wave is excited by an L-mode EM pump wave while ECH Wave is excited by an X-mode EM pump wave in the perpendicular case.

extract detailed information on particle dynamics which is normally very difficult to measure with a sufficient time resolution. On the right panels in Figure 14, plotted are the time history of the particle kinetic energy in the simulations. In both the Langmuir wave and ECHW cases, the particle thermal energy increases exponentially according as the electric field E grows exponentially, until the electric field reaches the saturation. This initial exponential increase of the kinetic energy, however, does not actually cause the thermalization of electrons, but reflects the sloshing motion synchronizing with the electric oscillation of the ES wave. However, at the time of the wave saturation, those particles begin to be thermalized through phase-mixing. The rise in the particle thermal energy and the fall in the electric field intensity after the saturation show that the particles start to extract energy from the ES wave and are heated.

Examination of the thermal energy increase helps us to understand why the saturation levels of the electric field of the ES waves are much lower than those estimated by theory, and why the measured Langmuir wave intensity is lower than that of the ECHW. To confirm the result of the first single simulation on the growth rate and saturation levels, we ran a series of simulations with different frequencies of the pump EM wave. The simulation parameters for the simulation series are listed in Table 2. The result is shown in Figure 15. The solid and dashed lines show theoretical values of the LW and ECHW, respectively. Those of the LW and ECHW observed in the simulations are plotted by square and circular symbols, respectively. The agreement of the growth rates (Figure 15(a)) between theory and simulations were confirmed by this series of simulations.

<Plasma Parameters>

Speed of Light	c	50
Electron Plasma Angular Frequency	Π_e	2.0
Electron Cyclotron Angular Frequency	Ω_e	1.0
External Magnetic Field Strength	B_{ext}	1.0
Charge to Mass Ratio of Electrons	q_e/m_e	-1.0
Total Number of Electrons	N_p	32768
Parallel Thermal Speed of Electrons	$v_{th\parallel}$	1.0 10^{-4}
Perpendicular Thermal Speed of Electrons	$v_{th\perp}$	1.0 10^{-4}
Dielectric Constant	ε_0	1.0

<System Parameters>

Time Step	Δt	0.01
Grid Spacing	Δx	1.0
Number of Grids	N_x	2048

<Parameters of Injected EM Wave>

Angular Frequency	ω_0	5.0 ... 22.5
Wave Number (Mode Number)	k_0	33 ... 109
Wave Magnetic Field Strength	B_ω	0.5

Table 2 - Numerical parameters for a series of simulations presented in Figure 15

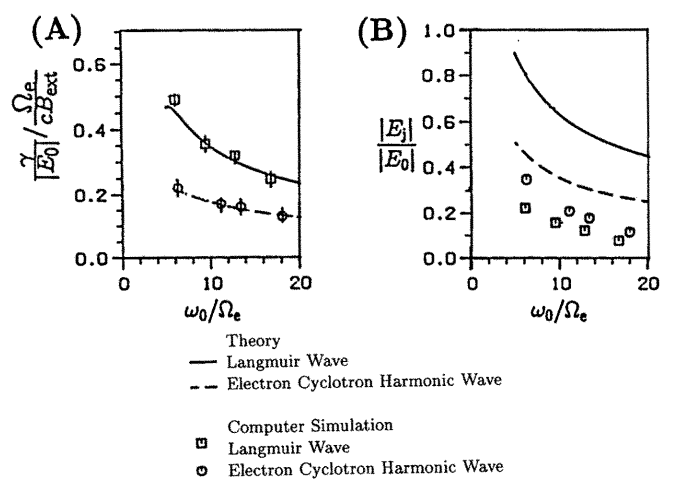

Fig. 15 - Comparison of the growth rates of the ES waves and their saturation levels between theory (indicated by lines) and computer simulations (indicated by symbols). The solid line and square symbols are for Langmuir Wave. The dashed line and circular symbols are for the ECHW.

On the other hand, the saturation levels observed in the series of simulations are much lower than the theoretical prediction shown in Figure 15(b). The larger gap between the theory and simulation for the Langmuir wave compared to the ECH wave results in the reversal of the saturation levels thereby contradicting the theoretical prediction. The saturation at lower intensity or at earlier time of interaction for the Langmuir waves turns out to be the result of the breakdown of the resonant condition (Eq.(2)). As seen in Figure 14, the plasma is heated by the nonlinearly growing ES wave leading to heating of the plasma. Therefore, the fact that the earlier saturation than predicted by the three-wave coupling theory should be related to the plasma heating. We then examined the change of the dispersion characteristics as a function of the electron temperature. The result shows that the dispersion relation of the Langmuir waves has higher susceptibility to the change of the electron temperature. Figure 16 shows the change of the dispersion relation in the ω-k diagrams when the electron temperature is doubled. As indicated in the figure, the increment of the frequency $\Delta\omega$, which represents the frequency mismatching, is larger for the LW than for the ECHW. The frequency mismatching given by $\Delta\omega = \omega_0 - \omega_1 - \omega_2$ influences the growth of the excited ES wave through [44],

$$\gamma = \sqrt{|\beta_1 \beta_2| E_0^2 - \Delta\omega^2} \tag{6}$$

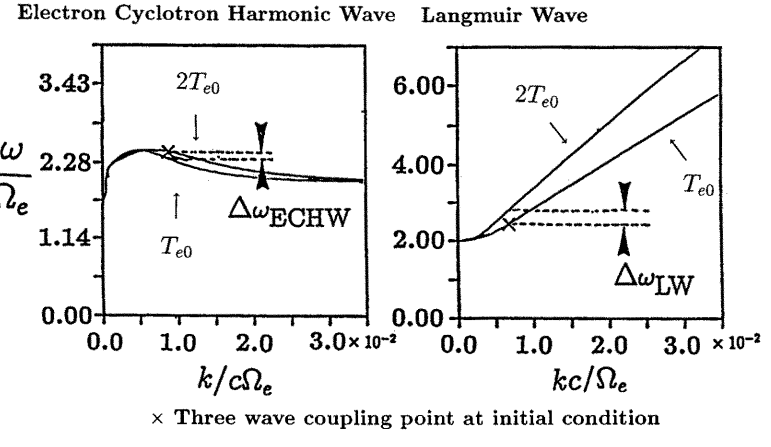

Fig. 16 - Comparison of the change of the dispersion characteristics of LW and ECHW due to doubling of the electron temperature. The quantity Dw gives a measure of the frequency mismatching from the resonant condition of the nonlinear three-wave coupling.

Therefore, the change of the dispersion relation, or the breakdown of the resonance condition for three-wave coupling due to plasma heating explains why the Langmuir waves reached saturation earlier and thereby stayed at a lower intensity than ECHW.

Another discrepancy concerning the nonlinear excitation of plasma waves by the microwave power beam revealed by the MINIX rocket experiment was the broad band nature of the excited Langmuir waves. The excited Langmuir waves did not show the line spectrum as predicted by the theory (Eq. (2)), but showed a broad spectrum. This can be understood in the light of the results of the computer simulation. The previous example of the simulation shows an effective plasma heating by the excited ES waves which self-quenches the wave-amplitude of the ES waves. This

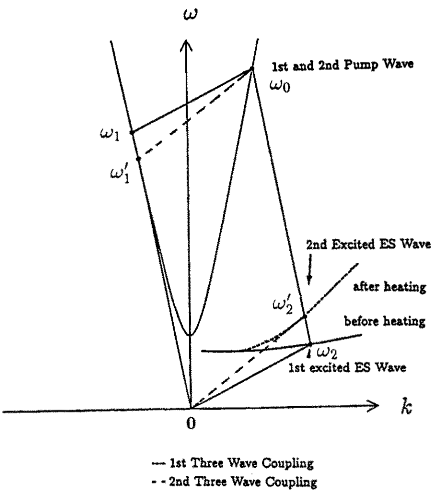

Fig. 17 - A schematic illustration of the change of resonance condition of the three-wave coupling involving Langmuir Waves. Due to the change of electron temperature, a new triplet (ω_0, ω_1 ', ω_2 ') is found automatically, thus leading to the frequency broadening.

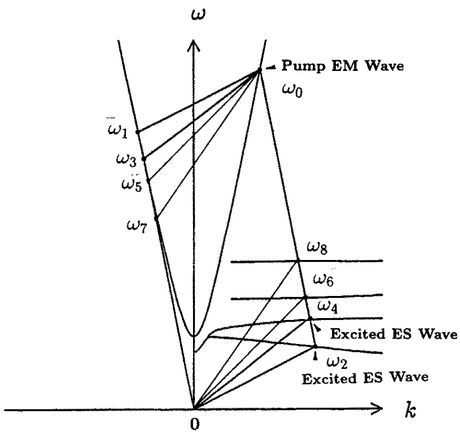

Fig. 18 - A schematic illustration of simultaneous nonlinear three-wave coupling by one EM pump wave feeding energy and momentum into multiple ECH waves.

means that the frequency and wave number of the triplet (ω_0, ω_1, ω_2) and (k_0, k_1, k_2) changes in time so that a new triplet automatically satisfies Eq. (2) for the heated plasma. A schematic illustration of this interpretation is given in Figure 17. Such sequential shift of the resonance frequency can explain the broad band nature of the observed Langmuir waves in the MINIX. Concerning the ECHW, another type of nonlinear three-wave coupling is possible for the electron cyclotron harmonic waves, as illustrated in Figure 18. In this case, multiple triplets (ω_0, ω_1, ω_2), (ω_0, ω_3, ω_4), (ω_0, ω_5, ω_6) can satisfy the energy and momentum conservation simultaneously as a result of multiple branches of the dispersion relations in the ω-k diagram. This feature can explain the MINIX multiple spectral peaks of the ECHW with a spacing of the order of the local electron cyclotron frequency.

As discussed above, even a simple one-dimensional computer simulation based on the particle model of the plasma turns out to be sufficiently effective to fill a gap between theory and experiment. Moreover the simulation solves an apparent discrepancy between the simple nonlinear theory and rocket experiment. Extending the simulation model from 1-D to 2-D, we are able to study the nonlinear interaction more realistically. Figure 19 is an example of such a 2-D simulation. Snap shots are shown of the spatial intensities of the pump wave (left upper panel), of the excited ES plasma waves (right upper panel) and of the thermal velocity of the plasma. The pump EM wave is radiated from the left boundary by an array of current sources placed on the left boundary, thus reproducing the spatially inhomogeneous intensity distribution of the MINIX microwave power beam. The ES waves shown in the upper right panel have already been damped in the vicinity of the antenna where the plasma is heated effectively.

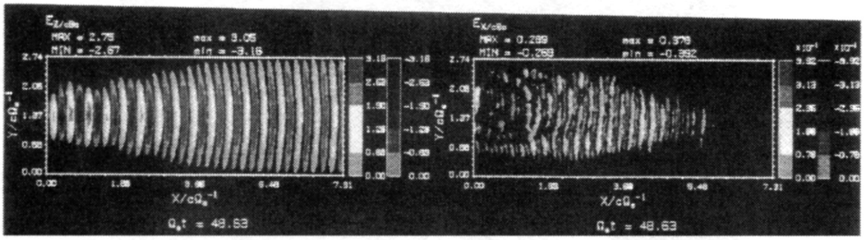

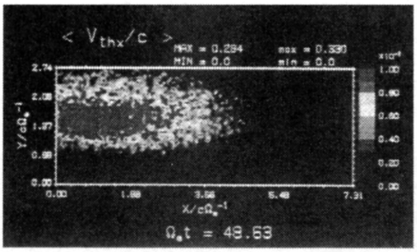

Fig. 19 - A set of the result of two-dimensional computer experiment by KEMPO on the nonlinear effects caused by the injected intense EM wave. The upper left panel shows the intensity contour of the electric field of the pump EM wave injected from the left boundary. The upper right panel shows the intensity of the excited ES waves. The lower left panel shows the spatial distribution of thermal speed of the plasma. It is interesting to note that the plasma electrons are heated in a region where the ES waves are intense.

The microwave power beam used for the future SPS has to pass through the magnetosphere and the ionosphere. In addition to the Ohmic heating and large-scale thermal instabilities discussed in Section 3, nonlinear excitation of electrostatic plasma waves is highly possible taking into account the theory, computer simulation and the rocket experiment MINIX. Though the power absorbed by these ES plasma waves and resultant plasma heating is very small, the impact of the microwave power beam onto the ionospheric plasma is not negligible. Nevertheless knowing the plasma wave characteristics excited by the microwave power beam as well as the physical plasma process involved in the excitation, we should be able to avoid possible interference to the HF communication network.

6. Application of Microwave Power Transmission to Microwave-Driven Airplane

In the late 1980's, a program to develop a long endurance high altitude platform called SHARP (Stationary High Altitude Relay Platform) was proposed in Canada [45]. The idea is to float an unmanned light-weight airplane for a long period, circling at an altitude of about 21 km for the purpose of relaying radio communications signals over a wide area. To maintain the platform floating for weeks or months, a fuel-less airplane powered by microwave energy transmitted from the ground was proposed and experimented on [46]. On September 17, 1987, a 1/8-scale prototype SHARP flew on beamed microwave power for 20 minutes at an altitude of about 150 m. Figure 20 shows a photo of the prototype SHARP with a 4.5 m wingspan. The microwave beam was transmitted by a 4.5 m diameter parabolic antenna transmitting 10 kW microwave with a

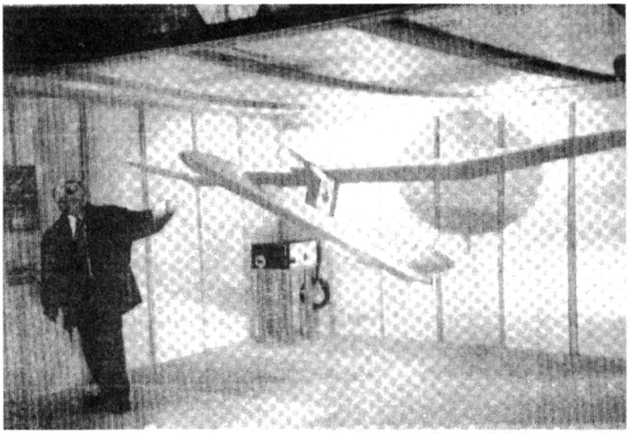

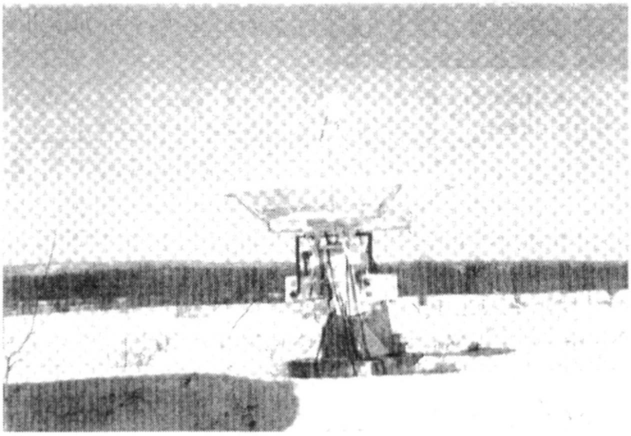

Fig. 20 - A 1/8-scale SHARP Airplane and a parabolic antenna which will be used for 1/4-scale SHARP experiment.

frequency of 2.45 GHz. Two water-cooled magnetrons each with 5 kW output power were used. The parabolic antenna mechanically tracked the airplane which flew inside a 50 degree cone. The power density at the airplane altitude was 400 W/m^2. A dual polarization rectenna with two orthogonal linearly-polarized dipole arrays was developed. The rectenna diodes used in the first flight were Silicon Schottky diodes (HP2835). Its power handling capability was 1 W/element, and its microwave-to-DC conversion efficiency was about 70% [46]. The rectenna received sufficient power to feed 150W to the electric motor of the 4.1 kg weight SHARP airplane [46].

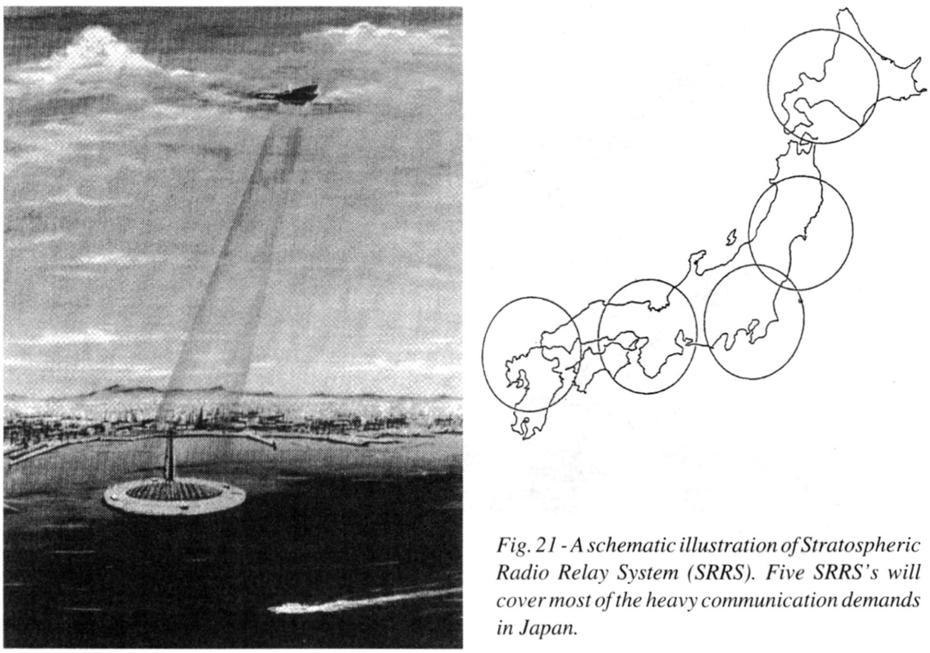

Fig. 21 - A schematic illustration of Stratospheric Radio Relay System (SRRS). Five SRRS's will cover most of the heavy communication demands in Japan.

A similar project was carried out in Japan in the early 1990's. The project was called Stratospheric Radio Relay Systems (SRRS), and was studied by a working group under the Ministry of Posts and Telecommunications of Japanese government [47]. The objectives of the SRRS are similar to those of Canadian SHARP. In the SRRS, it is planned to launch five such unmanned airplanes over Japan as depicted in Figure 21, so that these five platforms can cover most of areas where communication demands are heavy. In parallel with the SRRS working group, a microwave-driven airplane experiment was planned and conducted successfully on August 29, 1992 by a joint team organized by the present author [48]. The team members were from Kyoto University, Kobe University, Communications Research Laboratory, Nissan Motor Co. Ltd., Fuji Heavy Industries Ltd. and Toshiba Co. The experimental project was called MILAX meaning MIcrowave Lifted Airplane eXperiment, and was partly sponsored by ISAS of Japan. The MILAX airplane is a balsa-based light-weight (~ 4 kg) airplane with a 2.5 m wingspan and has a shape as shown in Figure 22. The MILAX flew successfully for 40 seconds (or 400 m distance over a straight course for car driving test) at an altitude of about 15 m. The testing scenery is shown in Figure 23. Because of the limits of the maximum microwave power (~ 1 kW) and of the aperture of the transmitting antenna (~ 1.2 m) , the flight altitude had to be as low as 15 m in order to guarantee the power density of 200 W/m^2 at that altitude. The microwave power beam was radiated toward the fuel-free MILAX airplane by an active phased array antenna. The MILAX active phase array transmitter was composed of five-stage Gallium-Arsenic (GaAs) semi-conductor amplifiers (see Figure 24), 4-bit digital phase shifters and circular microstrip antennas (see Figure 25). The transmitter is divided into 96 sub-arrays, each consisting of 3 antennas, one phase-shifter and one

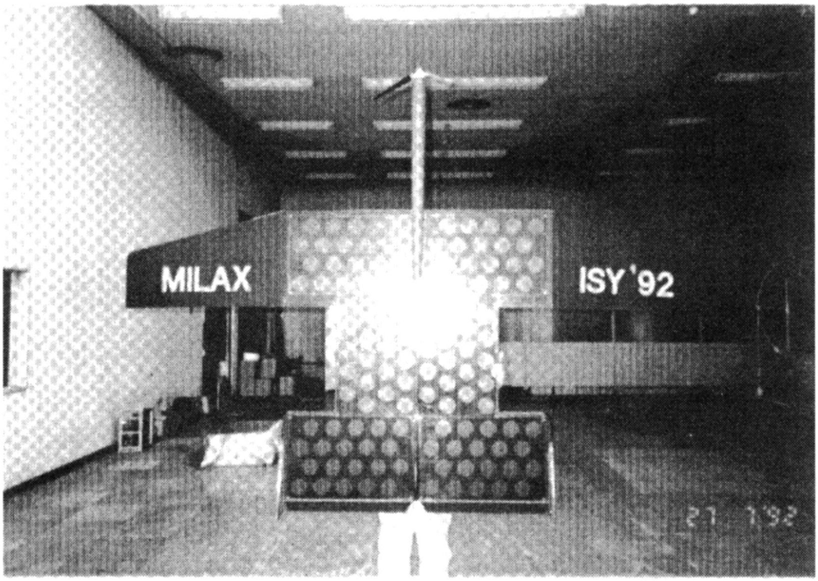

Fig. 22 - An outlook of MILAX airplane (Bottom side). Circular patches are microstrip antenna used for the antennas.

Fig. 23 - MILAX demonstration flight. The MILAX airplane flew only by the microwave power transmitted from the transmitter car running panelled to the airplane. The MILAX was conducted on Aug. 29, 1992 at Oppama driving test course of Nissan motor Co, Japan.

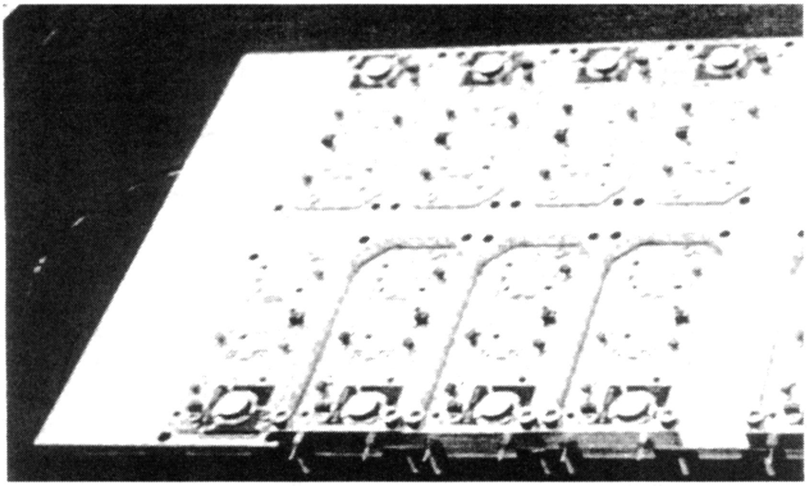

Fig. 24 - GaAs-based semiconductor amplifiers used in the MILAX. Each amplifier supplies 13 W microwave output.

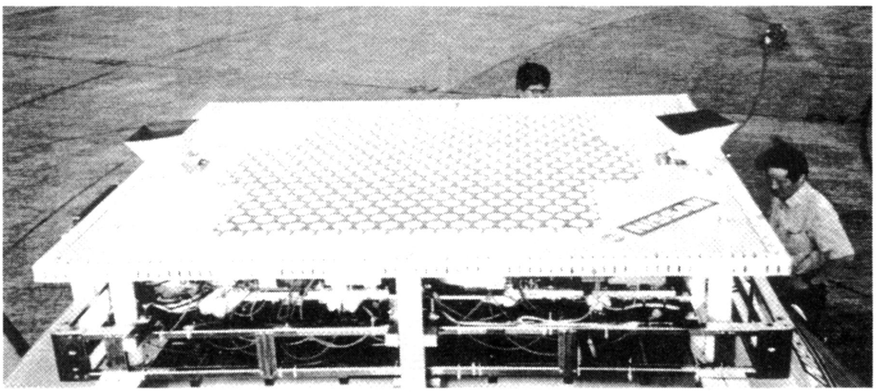

Fig. 25 - A view of the transmitting antenna array installed on the roof of a transmitter car. The antennas were of circular microstrip type.

GaAs amplifier. Each sub-array can supply 13 W microwave output resulting in the total radiation capability of 1.25 kW. The frequency used in the MILAX was 2.411 GHz in the ISM frequency band. The transmitter system was installed on the roof of a transmitter car (see Figure 25).

Six rectenna subarrays, each consisting of 20 rectennas are installed on the flat-bottom of the MILAX airplane. Prior to the development of the MILAX rectenna, several rectenna researches had been done in Japan [49, 50, 51]. Based on these studies, the receiving antennas used for the MILAX rectenna were not of the dipole-type, like these used in the JPL/Goldstone Ground-to-Ground Power Transmission Experiment and in the MINIX and SHARP, but were of a new type

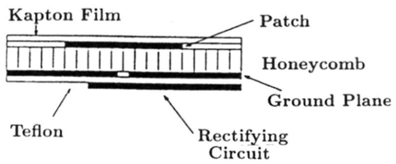

Fig. 26 - A microstrip circular antenna-based rectenna used for the MILAX project [50].

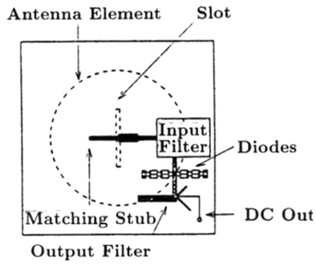

of microstrip circular patch antennas. The circular patch antennas have the advantage of a non-resonant nature at integer multiple harmonic frequencies, thereby having the capability of suppressing spurious radiation from the rectennas. The disadvantage of heavier weight as compared to dipole antennas was overcome by introducing a paper honeycomb structure [52], as shown in Figure 26. The diodes used for the MILAX rectenna are eight HP5082-2350 Schottky diodes in 2-series / 4-parallel combination. The power handling capability was 1 W per element, and the microwave-to-DC conversion efficiency was about 52 % [52].

The main reason of the adoption of the active phased array in place of a conventional parabolic antenna is its higher steerability of the microwave power beam. The power beam can be controlled and steered electronically in contrast to the mechanical control of a parabolic antenna. In the MILAX, we monitored the location of the MILAX airplane by two CCD cameras which were installed on the edge of the roof-transmitter antenna looking upward. In Figure 27, a system of identifying the location of the airplane is shown. A micro-computer, after recognizing the pattern

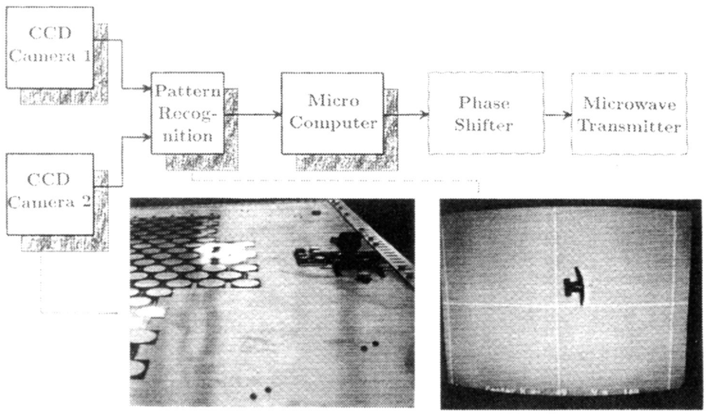

Fig. 27 - A computer-controlled beam steering system for microwave power transmission toward the MILAX airplane. The image of the airplane is captured by two CCD cameras installed on the roof of the transmitter car. Then the computer recognizes the airplane location and height by a pattern recognition software. According to the information on height and location, the computer controls the phase shifters of the microwave amplifiers of the active phased array.

of the airplane image and calculating the x-y coordinates and the altitude of the airplane, sends the control signals to the phase shifters of the microwave amplifiers so that the microwave beam is accurately directed toward the airplane. This system worked perfectly in the MILAX.

Though we adopted computer-control for steering the microwave power beam in the MILAX due to time and budget limitations, we have also attempted to develop the retro-directive beam control system. Figure 28 shows a photograph of a 90 W microwave power transmitter with the use of the retro-directive control method [53]. Seven dipole antennas are connected to semi-conductor microwave amplifiers. The 90 W microwave power transmitter has capability of transmitting the microwave power beam automatically in the direction of incoming pilot signals. A unique feature of the developed unit shown in Figure 28 is that it uses a new phase conjugate circuit (PCC) using asymmetric two pilot frequencies. The PCC used for the unit is shown in Figure 29. As we use two asymmetric pilot signals $\omega_0 + \Delta\omega$ and $\omega_0 + 2\Delta\omega$ instead of $\omega_0 \pm \Delta\omega$, we need no division of the phase ϕ_t of the pilot signal after the first mixer. Therefore we can determine the phase $\phi_1 t$ uniquely without the ambiguity of π radians.

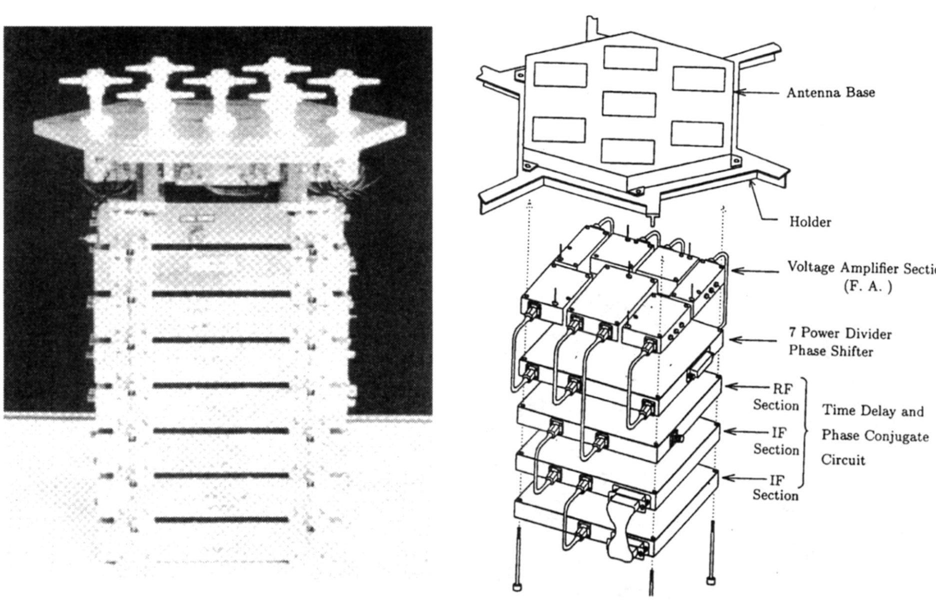

Fig. 28 - A 90 W microwave power transmitter unit composed of seven dipole antennas, seven GaAs semiconductor amplifiers and retrodirective phase conjugate circuits.

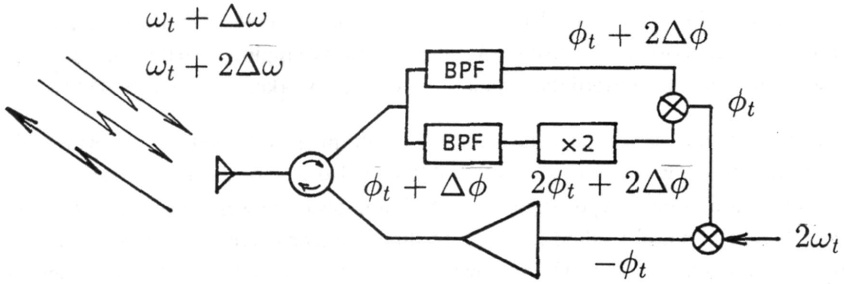

Fig. 29 - A new phase conjugate circuit used for the 90 W unit in Figure 28. Two pilot signals with asymmetric frequencies of $\omega_0 + \Delta\omega$ and $\omega_0 + 2\Delta\omega$ are used.

7. Other Recent Experiments on Microwave Power Transmission in Japan

On Feb. 18, 1993, a second rocket experiment of microwave power transmission between mother and daughter units was carried out by the S-520-16 sounding rocket [54, 55]. The rocket experiment was given the name of ISY-METS meaning Microwave Energy Transmission in Space during the International Space Year. The ISY-METS had objectives of investigating nonlinear effects of the high power microwave onto the ionospheric plasma in more or less a similar way to that of the MINIX. In this sense, the ISY-METS is an advanced version of the MINIX. However, it has another mission to verify a newly developed active phased array microwave transmitter which had been modified from that used in the MILAX in the space plasma environment. The total power of approximately 800 W was transmitted from the microstrip array

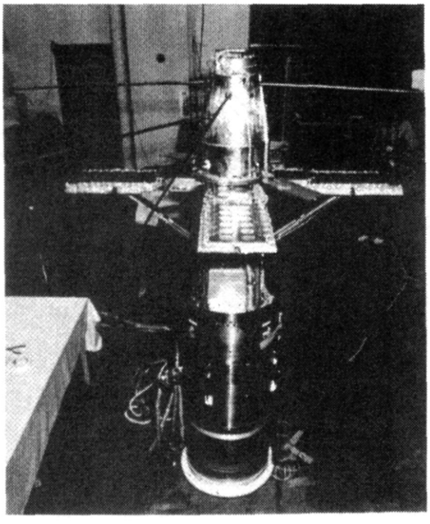

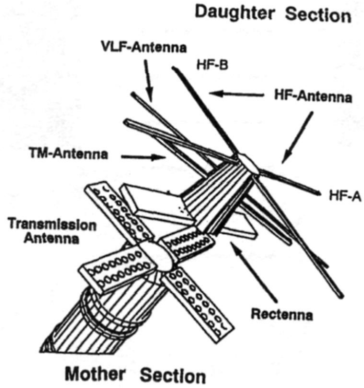

Fig. 30 - Picture and illustration of the payload section of the ISY-METS rocket experiment. Four deployed paddles mount 16 transmitting microstrip antennas each. The daughter unit carried diagnostic packages and rectennas with various sensors.

antennas mounted on four deployed paddles. The configuration of the transmitting antenna paddles and the sensors extended outward from the daughter unit are shown in Figure 30. The phase of the transmitted microwave from each antenna on the deployed paddle was controlled by the same 4-bit digital phase shifter as used in the MILAX. The phase shifters were controlled by an onboard computer providing a variable transmitted power density and direction of the microwave beam. Figure 31 shows an example of power concentration at a point of approximately 4.5 m away from the center of the transmitting antennas. Such power-concentrated points were determined by the computer using pre-set parameters and the onboard real-time data of the relative direction the daughter unit. Figure 32 shows a data set during a pre-flight test in the radio anechoic chamber. The left panel shows the antenna pattern of the microwave transmitter. The right panel shows the measured power at concentrated points which were varied from 1 m to 10 m from the transmitting antenna. The measured data are shown by the solid line in the figure. The dots in the same figure are the power density measured onboard the ISY-METS rocket during the flight; these measurements and agreed well with the pre-flight test values [55].

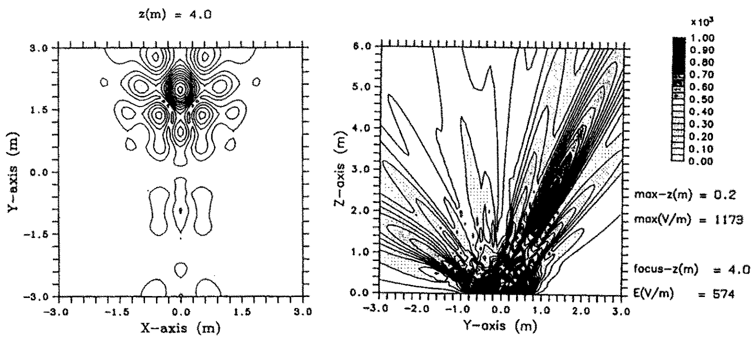

Fig. 31 - Computed power concentration map in the x-z and x-y plane, where the contour of the ISY-METS transmitting antenna is placed at x = 0, y = 0 and z = 0 in the x-y plane. In the specific example, the power-concentration point is set at (x, y, z) = (0 m, 2 m , 4 m)

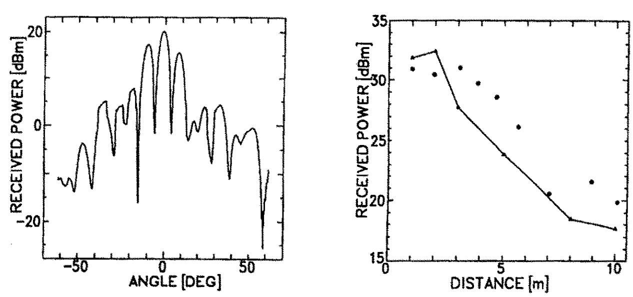

Fig. 32 - Antenna pattern of the ISY-METS microwave power transmitter (left), and the measured power (right) at power-concentrated points at distances from 0 m to 10 m. The solid line and dots represent the values measured in the pre-flight radio anechoic chamber, and in the flight in space, respectively.

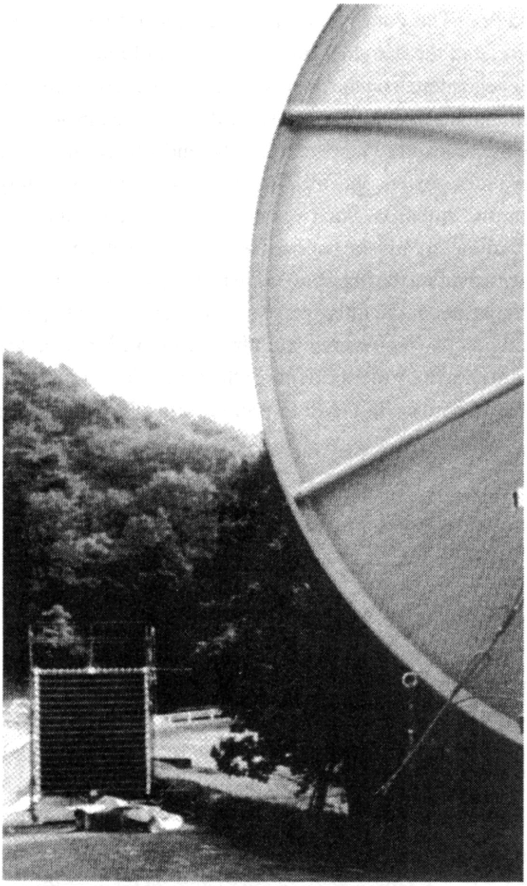

Fig. 33 - A photo showing a field experiment of MPT at Yamazaki Experimental Site of Kansai Electric Power Company Inc (KEPCI). The experiment is a joint collaborative research between Kyoto University, Kobe University and KEPCI (K^3 project).

Two types of rectennas were installed on the daughter unit. One was developed by a research group at Texas A&M University, while the other was by the CRL group. The former used an orthogonally placed pair of three dipole antennas, as used in the MILAX. The structure and configuration are found in Figure 9 and Figure 10 in [55]. The initial results of the ISY-METS rocket experiment are now under analyses and will be published in detail elsewhere.

Other applications of microwave power transmission have recently gathered interests in Japan in the practical world in addition to the academia. One of them is a small-scale ground-to-ground power transmission without wires toward a distant place where wired power distribution networks are either unavailable not or very poorly available. In order to collect fundamental data on microwave power transmission under varying weather conditions, the Kansai Electric Power Company Inc. began a collaborative field experiment with Kyoto University and Kobe University. Figure 33 shows a photo of the experimental site showing a parabolic antenna with a 3 m diameter driven by a 5 kW magnetron and a rectenna array of a size of 3.5 m x 3.2 m placed 42 m away from the parabolic transmitting antenna. The rectenna array was built by Kyoto University and is composed of 2304 rectenna elements. A preliminary test started in October, 1994 and is still being conducted to collect fundamental data on the characteristics of power transmission and reception by the system.

8. Discussion and Conclusion

The Tesla idea of wireless power transmission was revived by the NASA/DOE SPS studies program in the 1970's. Following the pioneering work on microwave power transmission by W. C. Brown, many engineers and scientists have conducted the related research and developed applications stimulated by the SPS studies program in

the US, former Soviet Union, France, Germany, Japan and other countries. However, even after the SPS boom subsided following the suspension of the SPS research in the US in 1981, both fundamental academic research and application-oriented developments and experiments in microwave power transmission have continued. Radio scientists have been a core of such research and development because the power transmission by radio inevitably involves problems in radio science such as those on antennas, rectennas, propagation characteristics and nonlinear interaction of microwave

power beam with plasmas and neutral environments. In this paper, we have emphasized the development of such studies after 1980 as studies before that time was well documented (e.g.[1]). Since 1980, many feasibility studies have been made and a variety of new ideas of utilization of microwave power transmission have been proposed. However, as far as the present author knows, very few experiments have actually been carried out except for those discussed in the present paper except for a laboratory-based development and research of rectennas.

There are many plans and proposals for MPT applications, e.g., a French plan of a medium-scale wireless power transmission (~ 100 kW, 3 km) on Reunion island, a proposal named WISPER (Wireless Space Power Experiment) in the US which aims at ground-to-space power transmission of the order of 100 kW, and a test project called ALASKA 21 which plans to transmit electric power via microwave to scattered villages in Alaska. As well as these, private industries have their own MPT projects, while national research institutes will continue fundamental researches.

In Japan, MITI (Ministry of Trade and Industry) has re-examined the SPS feasibility based on recently developed technologies after 1980. Japanese research groups at ISAS and national universities are accordingly pursuing a conceptual study on an orbiting 10MW-scale Power satellite called SPS2000 which beams down the electricity to equatorial countries [56] (Figure 34) and on a power satellite called PSS (Power Supplying Satellite) which feeds electricity of the order of 100 kW to other orbiting customers [57] (Figure 35).

In summary, microwave power transmission has been one of the interesting topics in radio science both technologically and scientifically However, the use of radio waves as a means of transmitting electric power and energy is still in a very immature phase. More research and development will be needed before the dreams of Hertz and Tesla became reality. Radio scientists and engineers have great challenges to face in this new field.

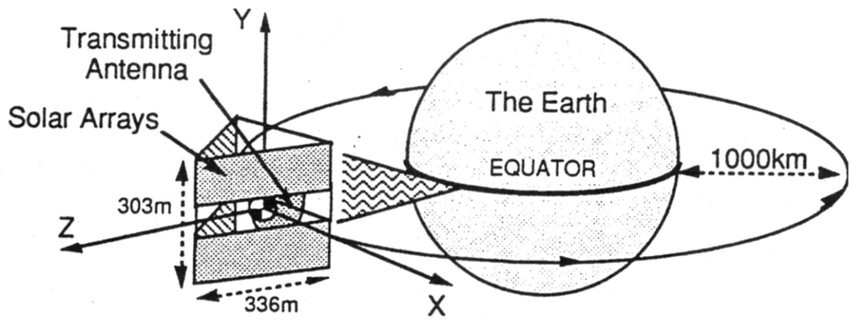

Fig. 34 - A concept of SPS2000 which will beam down electrical energy to equatorial countries from an orbiting satellite with a shape of triangular structure.

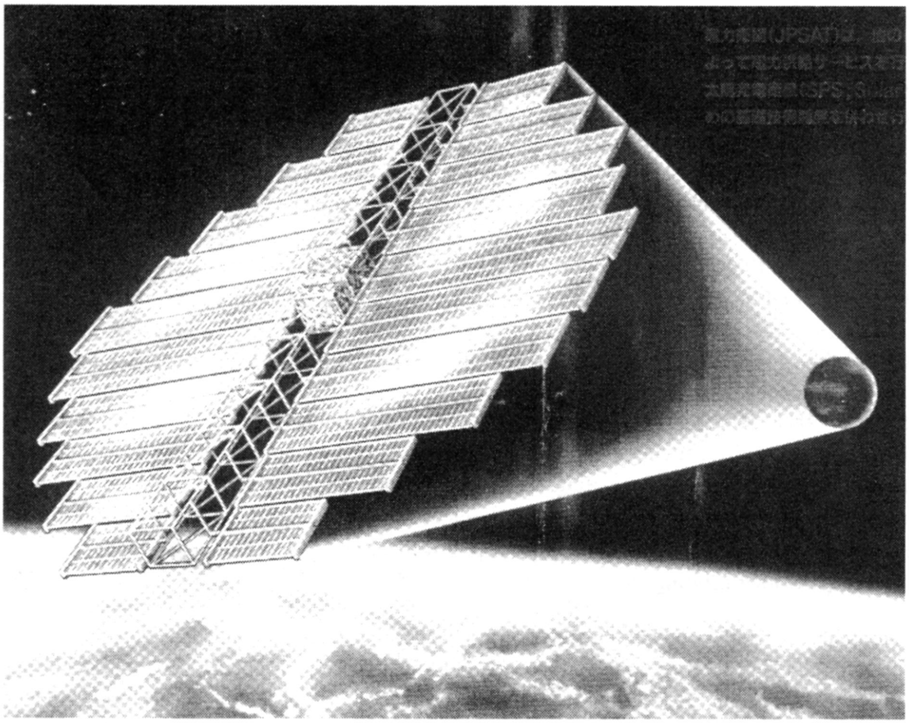

Fig. 35 - A concept of Power Supplying Satellite. A 100 kW power will be transmitted to customer satellites.

Acknowledgments

I would like to express my thanks to N. Kaya of Kobe University for his collaboration on this topic for many years. Without his contribution most of the experimental projects described in this paper would not have been successful. I also thank N. Shinohara, T. Miura and K. Miwa for their help in preparing this manuscript, and D. Summers for his careful reading of the manuscript.

References

[1] W. C. Brown, The history of Power transmission by radio waves, IEEE transaction on microwave theory and techniques, MTT-32, 1230-1242, 1984.

[2] I. C. Maxwell, Treatise on Electricity and Magnetism, Dover Publications (reprinted), New York, 1954.

[3] H. Hertz, Electric Waves, MacMillan and Co., New York, 1893.

[4] G. Marconi, Nozioni Elementari de Radio Telegrafia, Ufficio Marconi, Roma, 1916.

[5] R. A. Fessenden, Wireless Telephony, 25th annual convention of the American Institute of Electrical Engineers, Atlantic City, NJ, June, 1908.

[6] J. S. Belrose, Fesssenden and the Early History of Radio Science, The Radio Scientist and Bulletin, URSI, 5, 94-110, 1994.

[7] N. Tesla, The transmission of electric energy without wires, The thirteenth Anniversary Number of the Electrical World and Engineer, March 5, 1904.

[8] N. Tesla, Experiments with Alternate Current of High Potential and High Frequency, McGraw Pub. Co., N.Y., 1904.

[9] A. W. Hull, Effect of uniform magnetic field on the motion of electrons between co-axial cylinder, Phys. Rev., 18, 31-57, 1921.

[10] K. Okabe, Generation of Ultra short wavelength electromagnetic waves by magnetic with divided anodes, J. Institute of Electrical Engineering of Japan, 49, 284-290, 1928.

[11] H. Yagi and S. Uda, Feasibility of Electric Power Transmission by Radio Waves, Third Pan-Pacific academic conference, Tokyo, 1926.

[12] R. H. Varian and S. F. Varian, A high-frequency oscillator and amplifier, J. Appl. Phys., 10, 321, 1939.

[13] S. Nakajima and S. Yamazaki, Application of high power magnetron at Naval Research Laboratory during World War II time (in Japanese), History of Electronic Tubes, Ohm Pub. Co., Japan, 157-165, 1987.

[14] W. C. Brown, Experiments involving a microwave beam to power and position a helicopter, IEEE Trans. Aerosp. Electron. Systems, AES-5, No.5, 692-702,1969.

[15] W. C. Brown, Thermionic diode rectifier, in Microwave Power Engineering, vol. 1, E. C. Okress, Ed., N.Y. : Academic, 295-298 , 1968.

[16] W. C. Brown, The combination receiving antenna and rectifier, in Microwave Power Engineering, vol. II, E. C. Okress, Ed. N. Y.: Academic, 273-275, 1968.

[17] W. C. Brown, Progress in the design of rectennas, J. Microwave Power, vol.4, 168-175, 1969.

[18] R. M. Dickinson and W. C. Brown, Radiated microwave power transmission system efficiency measurements, Tech-Memo 33-727, Jet Propulsion Lab., Cal. Inst. Technol., March 15, 1975.

[19] Final Proc. Solar Power Satellite Program Rev. DOE/NASA Satellite Power System Concept Develop. Evaluation Program, Conf.-800491, July, 1980.

[20] P. E. Glaser, Power from the Sun, Science, 162, 857-886, 1968.

[21] F. W. Perkins and R. G. Roble, Ionospheric heating by radio waves : Predictions for Arecibo and the Satellite Power Station, J. Geophys. Res., 83, 1611-1624, 1978.

[22] L. M. Duncan and J. Zinn, Ionosphere-Microwave interactions for Solar Power Satellite, Los Alamos Scientific Lab. Report, LA-UR-78-758, March 1978.

[23] L. H. Holway and G. Meltz, Heating of the Laser ionosphere by powerful radio waves, J. Geophys. Res., 78, 8402-8408, 1978.

[24] L. M. Duncan and W. E. Gordon, Final Report, Ionosphere / Microwave beam interaction study, Rice University, Houston, TX, Final Report NAS9-15212, Sept., 1977.

[25] C. M. Rush, SPS simulated effects of ionospheric heating on the performance of telecommunication systems

: a review of experimental results, Space Solar Power Review, 2, 355-366, 1980.

[26] S. Basu, S. Bau, A. L. Johnson, J. A. Klobuchar, and C. M. Rus, Preliminary results of scintillation measurements associated with ionospheric heating in overdense and underdense modes, Geophys. Res. Lett., 7, 609-612, 1980.

[27] F. W. Perkins and E. J. Valeo, Thermal self-focusing electromagnetic waves in plasmas, Phys. Review Lett., 32, 1234-1237, 1974.

[28] J. E. Drummond; Thermal stability of Earth's ionosphere under power transmitting satellites, IEEE Transactions of Plasma Science, PS-4, 228, 1976.

[29] G. D. Thome and F. W. Perkins, Production of ionospheric striations by self-focusing of intense radio waves, Phys. Rev. Lett., 32, 1238-1240, 1974.

[30] L. M. Duncan and R. A. Behnbe, Observation of self-focusing electromagnetic waves in the ionosphere, Phys. Rev. Lett., 41, 998, 1978.

[31] B. L. Cragin, J. A. Fejer and R. L. Showen, Theory of coherent parametric instabilities excited by two or more pump waves, Geophys. Res. Lett., 5, 183-186, 1978.

[32] R. L. Showen, L. M. Duncan, and B. L. Gragin, Observations of plasma instabilities in a multiple pump ionospheric heating, Geophys. Res. Lett., 5, 187-190, 1978.

[33] H. Matsumoto, Theory of nonlinear interaction of SPS microwave with the ionosphere (in Japanese), Report of Inst. Space Astro. Science, Univ. of Tokyo, 15, 407-430, 1979.

[34] H. Matsumoto, Numerical estimation of SPS microwave impact on ionospheric environment, Acta Astronautica, 9, 493-497, 1982.

[35] H. Matsumoto and T. Kimura, Nonlinear excitation of electron cyclotron waves by a monochromatic strong microwave, Space Power, 6, 187-191, 1986.

[36] M. Nagatomo, N. Kaya and H. Matsumoto, Engineering aspect of the microwave ionosphere nonlinear interaction experiment (MINIX) with a sounding rocket, Acta Astronautica, 13, 23-29, 1986.

[37] N. Kaya, H. Matsumoto, S. Miyatake, I. Kimura, M. Nagatomo and T. Obayashi, Nonlinear interaction of strong microwave beam with the ionosphere, Space Power, 6, 181-186, 1986.

[38] I. Kimura, H. Matsumoto, N. Kaya and S. Miyatake, Plasma wave excitation by intense microwave transmission from a space vehicle, Advances in Space Research, 8, 291-294, 1988.

[39] N. Kaya and H. Matsumoto, Space chamber experiments of ohmic heating by high power microwave from the Solar Power Satellite, Geophys. Res. Lett., 8, 1289-1292, 1981.

[40] H. Hirata, Nonlinear wave-wave-particle interaction induced by intense EM waves in a magnetized plasma, Master Thesis (supervised by H. Matsumoto), Kyoto Univ., 1989.

[41] H. Matsumoto, H. Hirata, Y. Hashimoto and N. Shinohara, Theoretical analysis of nonlinear interaction of intense electromagnetic wave and plasma waves in the ionosphere (in Japanese), Trans. IEICE on Communications, vol. 78-B-II, March, 1995.

[42] H. Matsumoto, Computer experiment of space plasmas, Computer Space Plasma Physics, Simulation Techniques and Software, ed. by H. Matsumoto and Y. Omura, Terra. Sci. Pub. Co., Tokyo, 3-18, 1993.

[43] H. Matsumoto and Y. Omura, Particle simulation of electromagnetic waves and its application to space plasma, Computer Simulation of Space Plasma, ed. by H. Matsumoto and T. Sato, Terra Sci. Pub. Co. Tokyo, 43-102, 1985.

[44] for example, T.Taniuchi and K.Nishihara, Non-linear Waves (in Japanese), Iwanami Pub.Co., pp.116-134, 1977.

[45] G. W. Jull, A. Lillemark and R. M. Tunner, SHARP: Telecommunications Missions and Systems, Proceedings IEEE Globecom 85, 955-959, 1985.

[46] J. J. Schlesak, A. Alden and T. Ohno, A microwave powered high altitude platfome, IEEE MTT International Microwave Symposium, N.Y. Vol.I 283-286, 1988.

[47] Report of Studies on Stratospheric Radio Relay Systems, SRRS Working Group, Ministry of Postage and Communications, March 1991.

[48] H.Matsumoto, N. Kaya, M. Fujita, T. Fujiwara and T. Sato, Microwave Lifted Airplane Experiment with active phased array antennas, to be submitted to IEEE Trans. MTT, 1995.

[49] S. Adachi and Y. Shimanuki, Theoretical and experimental study on rectenna array for microwave power transmission, Space Solar Power Review, 5, 127-129, 1985.

[50] K. Itoh, Y. Akiba and Y. Ogura, Fundamental study on SPS rectenna printed ona sheet of Copper Glad Laminate, Space Solar Power Review, 5, 149-162, 1985.

[51] K. Itoh, T. Ohgane adn Y. Ogawa, Rectenna composed of circular microstrip antenna, Space Power, 6, 193-198, 1986.

[52] Y. Fujino, M. Fujita, H. Sawada and K. Kawabata, A rectenna for MILAX, 12th Space Energy Symposium, ISAS, Tokyo, March, 1993.

[53] H. Matsumoto, N. Kaya, N. Nagatomo, T. Hashizume,and K. Nakatsuka, Feasibility Study on Retrodirective System for METS, The Sixth ISAS Space Energy Symposium, 24, March 1987.

[54] H. Matsumoto and N. Kaya, Initial results of ISY-METS rocket experiment (in Japanese), RASC report Kyoto University, May, 1993.

[55] R. Akiba, K. Miura, M. Hinada, H. Matsumoto and N. Kaya, ISY-METS rocket experiment, The ISAS Report No.652, 1-14, September, 1993.

[56] M. Nagatomo, 10 MW Satellite Power System: A space station mission beyond 2000, Space Power 6, 299-305, 1986.

[57] H. Matsumoto, N. Kaya, S. Kinai, T. Fujiwara and J. Kochiyama, A feasibility study of Power Supplying Satellite (PSS), Space Power, 12, 1-6, 1993.